

PCCP

Accepted Manuscript



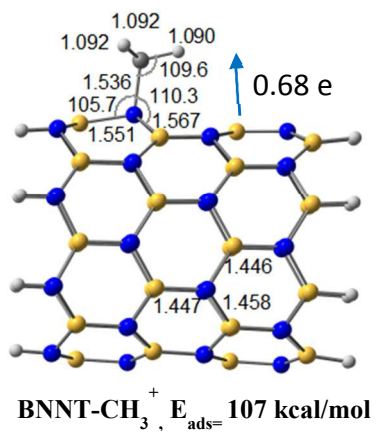
This is an *Accepted Manuscript*, which has been through the Royal Society of Chemistry peer review process and has been accepted for publication.

Accepted Manuscripts are published online shortly after acceptance, before technical editing, formatting and proof reading. Using this free service, authors can make their results available to the community, in citable form, before we publish the edited article. We will replace this *Accepted Manuscript* with the edited and formatted *Advance Article* as soon as it is available.

You can find more information about *Accepted Manuscripts* in the [Information for Authors](#).

Please note that technical editing may introduce minor changes to the text and/or graphics, which may alter content. The journal's standard [Terms & Conditions](#) and the [Ethical guidelines](#) still apply. In no event shall the Royal Society of Chemistry be held responsible for any errors or omissions in this *Accepted Manuscript* or any consequences arising from the use of any information it contains.

Graphical abstract



Site and chirality selective chemical modifications of boron nitride nanotubes (BNNTs) via Lewis acid/base interactions

Rajashabala Sundaram^{1,2}, Steve Scheiner², Ajit K. Roy³ and Tapas Kar^{2*}

¹School of Physics, Madurai Kamaraj University, Madurai-625021, Tamilnadu, India

²Department of Chemistry and Biochemistry, Utah State University, Logan, Utah 84322-0300, USA

³Materials and Manufacturing Directorate, Air Force Research Laboratory, Wright-Patterson Air Force Base, OH 45433, United States

ABSTRACT: The pristine BNNTs contain both Lewis acid (boron) and Lewis base (nitrogen) centers at their surface. Interactions of ammonia and borane molecules, representatives of Lewis base and acid as adsorbates respectively, with matching sites at the surface of BNNTs, have been explored in the present DFT study. Adsorption energies suggest stronger chemisorption (about 15-20 kcal/mol) of borane than ammonia (about 5-10 kcal/mol) in both armchair (4,4) and zigzag (8,0) variants of the tube. NH₃ favors (8,0) over the (4,4) tube, whereas BH₃ exhibits the opposite preference, indicating some chirality dependence on acid-base interactions. A new feature of bonding is found in BH₃/AlH₃-BNNTs (at the edge site) complexes, where one hydrogen of the guest molecule is involved in three-center two-electron bonding, in addition to dative covalent bond (N: → B). This interaction causes a reversal of electron flow from borane/alane to BNNT, making the tube an electron acceptor, suggesting tailoring of electronic properties could be possible by varying strength of incoming Lewis acids. On the contrary, BNNTs always behave as electron acceptor in ammonia complexes. IR, XPS and NMR spectra show some characteristic features of complexes and can help experimentalists to identify not only structures of such complexes but also the location of the guest molecules and design second functionalizations. Interaction with several other neutral BF₃, BCl₃, BH₂CH₃ and ionic CH₃⁺ acids as well as amino group (CH₃NH₂ and NH₂COOH) were also studied. The strongest interaction (> 100 kcal/mol) is found in BNNT-CH₃⁺ complexes and H-bonds are the only source of stability of NH₂COOH-BNNT complexes.

Corresponding author: Email: tapas.kar@usu.edu, Fax: 1-435-797-3390

INTRODUCTION

In 1923, G. N. Lewis proposed a generalized theory¹ of acid and base that allows chemists to predict a wider variety of acid-base reactions than Brønsted-Lowry's proton (H^+) theory. According to his definition a base is an electron pair donor while the acid accepts that pair, resulting in a coordinate covalently bonded compound, also known as a Lewis adduct. A common and widely used example of Lewis adduct in chemistry textbooks is ammonia borane (NH_3-BH_3) where ammonia (NH_3) donates a lone pair of electrons to the vacant p-orbital of borane. This bond is well known as a dative covalent bond and is represented as $H_3N \rightarrow BH_3$. The donating electron pair from base need not to be a lone pair, but can also be a pair of electrons in π -bonds. Acid-base reaction is one of the key components of chemical reactions and a wide range of chemicals (non-metal to metal in organic and inorganic chemistry) are involved in this process. Recent development of nanomaterials raised curiosity on how such nanomaterials can act as acid or base.

Since many boron and nitrogen containing compounds individually exhibit acid and base properties, respectively, then how will they behave when both are present in the same materials? If they show individual characteristics in such materials then what characteristics would they exhibit and how will those differ from simple Lewis acid-base adducts? Boron nitride nanotube (BNNTs) represent one such material and we explore acid and base properties by allowing BN-tubes to interact with guest acid and base molecules. Prior to proceed with our study, we briefly summarize structure, properties and chemical modifications of BNNTs.

Boron nitride nanotubes (BNNTs) were predicted in 1994^{2,3} and in the following year experimentally realized by arc-discharge method⁴. This pioneering experimental study initiated further development of synthetic methods of BNNTs by several groups⁵⁻¹⁰. Although BNNTs are structurally similar to their organic cousin carbon nanotubes (CNTs)^{11,12}, they exhibit extraordinary mechanical properties, larger thermal conductivity, higher field emission property, higher resistance towards oxidation and thermal stability than CNTs^{13,14}. These properties elevated the importance of BNNTs as a promising and attractive candidate for innovative applications in various fields of science and technology. Despite several similarities, nearly uniform electronic properties, insensitive to their chirality and diameters, makes BNNTs different from CNTs.

Chemical modifications not only allow tuning several properties of BNNTs, but also create new functionalized materials and have been an active research area¹⁵ since synthetic and purification methods were standardized to produce gram quantities¹⁶ of nanotubes. Such modifications includes substitutional doping, and covalent and non-covalent functionalization by a wide-range of chemicals at the surface. A recent theoretical study¹⁷ revealed that positively charged BNNTs can chemically adsorb CO_2 . If so, then one can make BNNTs as positively or negatively charged species. Guest Lewis acids and Lewis bases may play a role in such modifications of neutral BNNTs.

Intrinsic chemical properties of boron nitride nanotubes lie in their chemical composition, where boron atoms may behave as Lewis acid whereas nitrogen atoms may act as Lewis base. Due to the curvature of the tube, activities of those centers (due to pseudo- sp^2 hybridization and strain) may play an important role in covalent functionalization. Indeed, this property has been explored by two research groups^{18,19} where boron centers of BNNTs (in both multi-wall and single-wall tubes) were used as Lewis acid. The nitrogen atoms of tri-n-alkylamines and

phosphorous of tri-*n*-alkylphosphine, as Lewis base, forms an adduct with B center of multi-wall BNNTs and such complexes were found soluble in organic solvents¹⁸ with retention of the tube structure. However, such functionalization technique and bases were found inactive for single-wall BNNTs. A versatile strategy was proposed by Maguer et al.¹⁹ where nitrogen atoms of quinuclidine molecules were used for single- and multi-wall BN nanotubes and resulting adducts were soluble in different media including water. These experimental findings clearly suggest Lewis acid-base interaction plays a significant role in complex formation and open an avenue of wet chemistry of BNNTs.

However, fundamentals of such reaction processes, such as effects on guest molecules, interaction strengths, selectivity at the surface of the tube, dependence on the chirality, spectral characterization etc. are not yet explored. Knowledge of these factors not only will help to disentangle complicated experimental results, but will also provide fundamental ideas to advance research on chemical modifications of BNNTs. To understand and reveal characteristics of BNNTs toward acids and bases, we theoretically investigate single-wall BNNTs and different adsorbates at the surface of tubes. We first concentrate on the interaction with NH₃ (as base) and BH₃ (as acid), critically analyze these results, especially spectroscopic characterization. Then, other acids and bases are considered to determine the effects of derivatization.

Models and Computational Methods:

Covalent chemical modifications at the surface of zigzag tubes have mostly received attention in reported theoretical investigations¹⁵. Since the armchair configuration is also observed, both types of tube were considered to assess effect of chirality on the adsorption of NH₃, BH₃ and other acids/bases, and to estimate the strength of Lewis acid-base interaction and other properties of resulting complexes. As representatives of armchair and zigzag tubes, (4,4) and (8,0) BNNT, respectively were chosen in the present investigation. These molecular models, most commonly used in previous theoretical studies, contain 32 boron and 32 nitrogen atoms; tips were saturated with hydrogens to avoid dangling bonds. We also included larger tube models to verify the effect of length and diameter on the interaction with acid and base.

Previous studies²⁰⁻²⁴ on the interaction between NH₃ or its derivatives and BNNTs were mostly modeled at the middle of the tube surface and a periodic boundary condition (PBC) was applied. Since active sites are also possible at or near the edges, such periodic models are missing the edge-effects on the adsorption properties. Moreover, periodic boundary conditions cannot be applied to mimic edge functionalizations due to interruption of translational symmetry. Thus, the molecular model seems an appropriate approach at present, unless some new modeling technique is evolved. In our models, adsorbents were placed at various sites, starting from one end of the tube and progressively moved to the other end, covering all possible adsorption sites. To identify those acid and base centers of the tubes, a numbering scheme (Scheme I) is used, where B stands for acid center and number 1 to 4 indicates the location at the surface of the tubes. Similarly the base centers are indicated using N1 to N4.

The B3LYP variant of density functional theory (DFT)^{25, 26} was used to include correlation effects. A double- ζ quality 6-31G* basis set augmented with polarized d-functions for all heavy atoms was used. Several previous studies²⁰⁻²⁴ on BNNTs used a similar basis set. Basis functions without a set of diffuse sp-functions for electronegative atoms are inadequate, especially for interaction energy. So an additional set of diffuse sp-functions was added to the 6-31G* basis function. Geometries of pristine and chemically modified BNNTs were fully

optimized without any symmetry restriction using both 6-31G* and 6-31+G* basis sets, followed by vibrational analyses that insure the identification of true minima.

Adsorption energies (E_{ad}) represent the energy difference between the complex and constituents and are obtained using the following equation (eq 1), where E is the electronic energy.

$$E_{ad} = E(\text{BNNT-NH}_3/\text{BH}_3) - (E(\text{BNNT}) + E(\text{NH}_3/\text{BH}_3)) \quad (1)$$

For an attractive or favorable interaction, the adsorption energy (also termed as interaction or complexation energies in following description) is negative, otherwise it is positive. Some research groups use this quantity as it is obtained in eq 1, while others use negative of E_{ad} for attractive interaction. We followed the latter terminology, i.e., E_{ad} is positive for attractive interaction (exothermic process) and the complex is stable. All adsorption energies are corrected for basis set superposition error (BSSE), where one unit uses basis sets of others in complex and vice versa) using the counter-poise (CP) method²⁷.

Besides structural and energetic information of the complex formation, IR, XPS and NMR characterization were included in this study. Calculated harmonic vibrational frequencies are normally slightly higher than experimental values (even for more accurate methods, such as MP2, CCSD etc, as well as for larger basis sets, and anharmonicity corrections) and a scale factor is commonly used to better correspond with experimental spectra. For example, a value of 0.960 is recommended for B3LYP/6-31G* methods²⁸. Natural population analysis (NPA) and natural bond orbital (NBO) analyses^{29, 30} were performed to obtain charge distribution and nature of bonding in the complexes. Binding energies (BE) of the 1s orbital (for XPS spectra) of B and N atoms were estimated from the negative of core orbital energies from NBO data. For NMR spectra, the GIAO method^{31, 32}, most commonly used for wide range of compounds, was used to obtain chemical shielding constant (σ_{iso}) and chemical shift (δ) of ¹¹B and ¹⁵N.

All calculations were performed using the Gaussian-09³³ code. Models of BNNTs and modified BNNTs were obtained using Chemcraft³⁴ software, which was also used to generate figures for geometry and vibrational analyses.

RESULTS AND DISCUSSION

Several interactions of ammonia and borane at the surface of BNNT are possible and those are: (a) via N-H...N(BNNT) hydrogen bonding where one of the hydrogens of ammonia approach the N atoms of the tube, (b) B-H-B(BNNT) three-center two-electron (3c-2e) bonding³⁵ where one of the hydrogens of BH₃ is also shared by one of the boron atoms of BNNTs, (c) H atom of NH₃ approaching the middle of the BN-hexagonal ring, representing π -cation interaction and (d) formation of covalent dative N: \rightarrow B bond where B(N) of adsorbents interact with N(B) atom of the tube. All attempts to optimize H-bonded as well as solely B-H-B 3c-2e bonded structures on top of BN hexagonal ring were not successful and optimization starting with any of those kinds of structures led to covalent dative bonded adducts in most cases. This is not surprising as the covalent interaction is the strongest among three interactions, and such complexes are global minima in the potential energy surface²⁰.

BNNTs-NH₃:

In the 64 atom molecular model of BNNT, basically there are four possible Lewis acid sites from one end of the tube to the other end as shown in Scheme I and incoming Lewis base (single NH_3 molecule) is attached to these four active centers, unlike previous studies²⁰⁻²³ where only one center at the middle of the surface was considered. The BSSE corrected B3LYP/6-31+G* fully optimized structures of those four (4,4)-BNNT- NH_3 are depicted in **Fig. 1**, along with most relevant geometric parameters at the adsorption site. To verify the effect of adsorption on BN bond distances far from active site, some of those BN distances are also given in figures. Adsorption energies (E_{ad}), with and without BSSE correction, are summarized in the first two columns of Table 1. As expected, counterpoise correction lowers the E_{ad} value by about 2.6-3.0 kcal/mol. Similar values were reported in an earlier work²³ using B3LYP/6-31G*. These results indicate non-CP corrected adsorption energies are overestimated by a meaningful factor that cannot be ignored in studying such interactions and BSSE correction is highly recommended while using similar basis functions. In the following discussions of adsorption energies, BSSE corrected energies $E_{\text{ad(}(\text{CP})}$ values are used.

All four (4,4)-BNNT- NH_3 complexes (1A-1D) exhibit almost constant adsorption energy at about 4.5 kcal/mol indicating all four sites, either near the edge or at the middle of the surface, are equally favorable. Interaction energy between ammonia and borane is 28.3 kcal/mol (BSSE corrected) at the same level of theory, which is close to the MP2/6-31+G* value of 28.1 kcal/mol and experimental estimate of 30.7 kcal/mol³⁶. Thus, a tubular and extended conjugated BN structure reduces the binding energy significantly. The newly formed B-N bond lengths are in the range of 1.724-1.733 Å, longer than in $\text{H}_3\text{N-BH}_3$ (1.682 Å at B3LYP/6-31+G*, 1.668 Å at MP2/aug-cc-pVDZ³⁷ and 1.658 Å (experimental)³⁸). Thus, the method used in the present study seems reasonably accurate in predicting energies and structures but computationally more efficient than expensive correlation methods.

The effect of ammonia adsorption on the BN tube structure is localized at the vicinity of the active sites which is reflected in lengthening only the adjacent three BN bonds by about 0.5 Å, i.e., change in double bond character (about 1.45 Å in pristine tube) to single bonds (~1.52 Å). Complexation causes slight (~3 mÅ) elongation of NH bonds of NH_3 . Based on these energies and distances, interaction between ammonia and (4,4) tube may be considered as weakly bound complexes. It is worth mentioning that such interactions cannot be termed physisorption, a phenomenon normally described for weaker van der Waal interactions.

Unlike in armchair tube, ammonia adsorption at the zigzag (8,0) tube (**Fig. 2**) strongly depends on the location of the B-site (see scheme I). The edge site (B1 in 2A), where acid center is connected to two N and one H atoms, is found preferable (stabilized the 2A complex by 11.4 kcal/mol) to 2B or 2C, where B-centers are located in the middle. The binding energy of 2A is more than double that of the armchair counterpart (1A-1D). The adsorption process is endothermic (repulsive) by 1.4 kcal/mol for the structure 2D, where B-center near the edge is surrounded by three N atoms. The strongest interaction between constituents in 2A is reflected in the B-N(H_3) distance, which is found the shortest (1.691 Å) among others (1.724 – 1.789 Å). Other bond parameters removed from the functionalized site are not perturbed noticeably by such interactions, indicating localized effect on the tube surface.

Previous studies on NH_3 adsorption at the surface of similar zigzag tubes, where adsorbate was considered in the middle of the tube surface, indicates chemisorption and the energy of association is about 10-12 kcal/mol^{20, 21, 23, 24} depending on the level of theory (PBE and PW91, and similar double-zeta quality basis functions) and periodic models. These energies

are higher by about 5-7 kcal/mol than the present values of about 4.5 kcal/mol (2B and 2C) as previous energies were not corrected for BSSE which inflated the energy by about 3 kcal/mol. Also the use of diffuse function, not considered in most previous studies, lowers the interaction energy by about 2.0 kcal/mol (Table S1). BSSE corrected interaction energy of 5.6 kcal/mol of (9,0)BNNT-NH₃ was obtained²⁴ by using the larger 6-311G* set for BNNT and Ahlrichs TZP for NH₃ with the B3LYP-D* dispersion correction Grimme method. Thus, the method and basis function used in the present study are highly reliable. Geometric parameters are not affected noticeably either by BSSE correction or the use of diffuse functions (S2-S3).

Wu et al.²⁰ reported the minimum energy path (MEP) for the adsorption of NH₃ on the middle of the (8,0) surface (PBC calculation) and estimated a barrier height of 2.7 kcal/mol. This estimate was not verified by vibrational analysis (imaginary frequency for the transition state). We could not locate transition states for any of these reactions and guess the process may follow a direct addition reaction without a transition state.

In summary, adsorption of ammonia depends on the location of the Lewis acid site. At the middle of the surface, both kinds of tube display same adsorption energy. However, edge sites make a difference in preference of adsorption. The boron atom bonded to two nitrogen atoms and a terminating hydrogen atom of zigzag tube is preferred. However, the boron surrounded by three N atoms near the edge of same tube is least favorable. Using DFT-based local reactivity descriptor, Saha et al.³⁹ reported that edge and near the edge of the (5,5) tube are most active nucleophilic and electrophilic sites. BSSE correction and use of diffuse function have importance in estimating interaction energy.

BNNTs-BH₃:

The interaction scenario is reversed in the BNNT-BH₃ complexes, where nitrogen atoms of the tube are used as base centers, not explored earlier. Similar to acidic B-sites, all four possible active nitrogen centers (scheme I) of the tube are used for anchoring single BH₃ molecule and the resulting complexes are shown in **Fig. 3** and 4, and adsorption energies in Table 1. The structure 3A that holds Lewis acid at the edge N1 site with an adsorption energy of 20.0 kcal/mol is found the most stable in (4,4)-BNNT-BH₃ complexes. The structural feature of 3A is unique in the sense that the stability is due to a B-H-B three-center two-electron (3c-2e) bond³⁵ in addition to the common dative covalent N:→B(H₃) bond found in other complexes. Such 3c-2e bonding is common in boron hydride chemistry⁴⁰. These two attractive forces bring the two units closer to each other compared to any other complexes. For example, the pertinent B-N bond is shortest (1.585 Å) among all structures considered in this study. The BH bond, participating in 3c-2e bond is significantly elongated from 1.194 Å to 1.326 Å, and the same H of BH₃ is 1.361 Å from the B atom adjacent to the N1 site. Such a close B-H distance is characteristic of B-H-B 3c-2e bonds, e.g. in diborane (B₂H₆), where the bridging H atom is 1.317 Å far from the boron atoms. The other indicator of B-H-B 3c-2e bond is the θ(BHB) angle, close to 90°, also found in the 3A complex. It may be worth mentioning that the B3LYP/6-31+G* dimerization energy of borane to diborane is 38 kcal/mol, where two B-H-B bonds are formed. Thus, the B-H-B bond in 3A contributes significantly.

Complexes 3B and 3C, obtained by moving BH₃ to the middle sites N4 and N2, respectively, are stabilized by 8.3 and 7.2 kcal/mol. In the former isomer, the N-B(H₃) distance of 1.804 Å is longer than in 3A and 3C complexes, and the standard BN single bond length. It is quite unusual that even with such larger separation of two units, their interaction is stronger than

any BNNT-NH₃ complexes where middle sites are active. Based on relevant geometric parameters, 3C exhibits much weaker 3c-2e BHB than in 3A. In addition the longer B-N distance than in 3A (1.629 vs 1.585) makes 3C less stable. Similar to 3B, 3D exhibits the longest N-B bond (1.828 Å) among all complexes, stabilized by about 7 kcal/mol.

Out of four possible attachment sites (N1-N4), adsorption of BH₃ at the edge (N1) and near-the-edge (N4) sites of (8,0)-BNNT are equally favorable. The E_{ad} (CP) value of about 14.5 kcal/mol is slightly more than double that of the other two isoenergetic 4C and 4D structures. Of the two most stable structures, 4B exhibits multi-center bonding (as in 3A) in addition to covalent N-B(H₃) bond, whereas 4A is stabilized only by the latter type covalent interaction, still both exhibit the same adsorption energy. At the two middle centers (N2 and N3), BH₃ adsorption is equally favorable. So the location of the Lewis base site of (8,0)-tube has a significant role in binding the Lewis acid.

Geometric parameters at the functionalized site of 4B slightly differ from those of 3A, which may be the reason for the smaller adsorption energy of 4B than 3A. For example, the relevant N-B distance in 4B is longer by 0.025 Å than in 3A, the existing B-H bond of 3c-2e interaction is less stretched in 4B than in 3A 0.011 Å. These factors cause both interactions to be weaker in 4B than in 3A, and hence lowers the adsorption energy by about 5 kcal/mol relative to 3A.

To verify the effect of tube length, a (8,0) BN-tube with 56B and 56N atoms was also studied and BSSE corrected adsorption energies along with structures are reported in **Fig. S4**. As expected, extension of the tube length from 7.2 to 13.7 Å has practically no effect on the adsorption energy either at the edge or at the middle sites. For example, E_{ad} values at the edge and middle sites of the longer (8,0)BNNT-NH₃ are 11.9 and 4.2 kcal/mol, respectively, and the corresponding energies for (8,0)BNNT-BH₃ are 14.2 and 6.9 kcal/mol, respectively. These values are within +/- 0.5 kcal/mol of those in the smaller 64 atom tube.

Ammonia adsorption energy decreases with the increasing diameter of the zigzag BN tube and such energy is smallest in the BN-sheet^{21, 23, 24}. The counterpoise corrected E_{ad} values for a larger (12,0)-BN tube (**Fig. S5**) follows the same trend for BH₃ also. The increase in diameter of 3.3 Å, from (8,0) to (12,0), lowers the BH₃ adsorption energy from 14.5 to 9.7 kcal/mol at the edge site, and from 6.9 to 4.4 kcal/mol at the middle site. Thus, smaller diameter tubes most likely form stable complex with guest acids and bases.

In summary, the Lewis base character of BNNT seems stronger than the Lewis acid character, as BH₃ (Lewis acid) adsorption energies are significantly higher than those of NH₃ (Lewis base). While the most favorable site for NH₃ is the edge of (8,0)-BNNTs, BH₃ opts for the edge of cousin (4,4)-BNNT, which can distinguish between two kinds of tubes. Besides (4,4)-BNNT-NH₃, in all other cases both NH₃ and BH₃ prefer edge or near the edge sites. Adsorption at the middle of the surface is energetically less favorable than the edge sites.

Deformation energies:

Since complex formation causes deformation of BNNTs, energies of such deformation (E_{Def}) were calculated by subtracting the energy of BNNT unit at the respective complex geometry from the energy of pristine tube. Similarly, E_{Def} of NH₃/BH₃ is the energy difference between the deformed structure in the complex and the fully optimized molecule.—Such deformation is associated with an energy rise and those are given in Table 1. Although the structural perturbation occurs only in the vicinity of acid/base interaction site, E_{Def} values are

noticeable. For ammonia complexes, deformation of both tubes cost about 18-19 kcal/mol, whereas NH_3 molecule is not deformed at all as indicated by its negligible deformation energies (about 0.1 kcal/mol). In contrast, significant structural changes occur in the BH_3 molecule. E_{Def} of BH_3 connected only through covalent bond as in 3B, 3D, 4A, 4C and 4D is 10-12 kcal/mol. But this number is more than double when it participates in an additional 3c-2e bond with tube (as in 3A, 3C and 4B). In contrast to NH_3 complexes, tube deformation is significantly less (about 3.5 kcal/mol) when it acts as base in BH_3 complexes where only a covalent dative bond is the source of interaction. Otherwise deformation energies (19-21 kcal/mol) are almost in the same range as noted in NH_3 complexes.

The changes in NH_3 and BH_3 molecules are not surprising and can be rationalized in terms of changing hybridization upon complexation. BH_3 is sp^2 hybridized and in complexes accepts the electron pair from the base N site to its vacant p-orbital (perpendicular to the plane, hybridization angle $\phi=90.0$, see **Fig. S6**) and tends toward a tetrahedral structure ($\phi=104.6$), i.e., convert from sp^2 to sp^3 hybridization. When one of the H atoms of BH_3 takes part in multicenter bonding, then additional deformation enhances the E_{Def} values. In contrast, NH_3 already possesses tetrahedral structure (S4, $\phi=111.2$) where the lone pair orbital is in the position of one arm of tetrahedral arrangement and interacts with the acid center of the tube without changing its hybridization (retains same ϕ angle), so there is no major change in structure except slight elongation of NH bonds.

The ripple surface of BNNTs, where N atoms (base sites) are pulled out from the tube surface while B atoms (acid sites) are pulled down, may be an important factor of complexation. (It may be noted that such ripple feature of the surface is easily visible in armchair tube, but not so obvious in zigzag tube. At first glance it may appear some N atoms are slightly below neighboring B atoms, but rotation of the tube along the axis of the tube shows those above the surface to the adjacent B atoms). In **Figs. S7-S9**, three hybridization angles of edge, middle and near-the-edge of B and N centers of pristine and functionalized tubes are shown. Such angles at the boron sites of pristine tubes are about $92 - 94^\circ$ (S5), supporting hybridization close to sp^2 . Covalent bond formation with ammonia should change these angles closer to the typical tetrahedral angle of 109.5° . Indeed, all ammonia complexes exhibit closer tetrahedral angles ($\sim 105^\circ$, **Fig. S8**) and it can be seen from **Figs. 1 and 2** that active B atoms are pulled up while the bonded 3 atoms of tube are pushed down. This may be the cause of larger deformation energy of all BNNT- NH_3 complexes.

In pristine tubes, hybridization angles of the active N atoms are larger than those of the B centers, where the two angles are about $4-6^\circ$ higher and the third one, perpendicular to the tube axis, is in the range of $100-106^\circ$ (S5). When these N atoms act as the anchoring site, N atoms are moved further up from their existing position. In those cases where only dative B-N bonds are formed with incoming Lewis acid (as in 3B, 3D, 4A and 4C) angles increase by about $2-6^\circ$ (**Fig. S9**). Since the N atoms shift in the favorable direction and the magnitude is not large, the deformation energy of 3-4 kcal/mol (Table 1) is small. However, in those cases where additional attractive 3c-2e interaction involves changes in angles and pertinent bond distances deformation energies are large. The BH_3 molecule, when attached to N sites, undergoes change in hybridization from sp^2 to sp^3 and the related change in hybridization angles (90° to about 104° , see **Fig. S6 and S9**) is the indicator for such a shift. Such large deformation is manifest in E_{Def} values around 23-26 kcal/mol.

NBO analyses:

In a previous section, the importance of pyramidal angles in the complex formation was described. At the edges, both B and N atoms are flexible, compared to their location at the middle. Smaller structural strain is one reason for their being more favorable acid/base sites. To gain further insight about the Lewis acid/base character of BNNTs and their interactions with external base/acid, natural bond orbital (NBO) analyses were performed on pristine and modified tubes. The salient NBOs are shown in **Fig. 5**, along with vacant p-orbital of BH_3 (B lp^* , electron pair acceptor orbital) and donor lone pair orbital (N lp) of NH_3 shown at the top of the figure. NBOs of (4,4) and (8,0)-BNNT, as expected, exhibit three types (B-N, B-H and N-H) of σ bonds, and representative NBOs of each case are shown in **Fig. 5**. The B-N π NBOs (again representative of several such bonds) depicted in the next row of the figure, indicates a slightly larger contribution at the N atom than the B atom, due to electronegativity difference.

A significant difference between (4,4) and (8,0) tubes occurs in the N lone pair (N lp) NBOs at the edge of the latter tube, which are not present in the analogous (4,4) tube. In the last row, the antibonding NBOs are shown, where only (8,0)-BNNT exhibits lp^* at the boron atoms located at the edge, again not present in the (4,4) tube. As expected, B makes a larger contribution than N to the BN π^* NBOs. Such differences are inherent in the atomic arrangements in these tubes. In the (4,4) tube, the edge contains 8 atoms, half B atoms and other half N atoms, in alternating B and N sequence. So both edges of armchair tubes exhibit the same atomic composition of B and N. In contrast, one edge of (8,0) or any zigzag tube contains boron atoms (B-rich-edge as shown in scheme I) and the other edge contains all N atoms (N-rich-edge). Such differences are a prime reason behind different chemical activities at the edges of these two kinds of tubes.

In the complexation, interaction takes place between donor (Lewis base) and acceptor (Lewis acid) and the strength of the interaction depends on the type of participating NBOs. In NH_3 -BNNT complexes, the donor is NH_3 and B sites are the acceptors. The situation reverses for BH_3 -BNNT complexes, where N of the tube acts as donor and BH_3 is the acceptor. The strongest interaction between Lewis acid and base originates from $\text{lp} \rightarrow \text{lp}^*$, as in ammonia borane (where the interaction energy is about 30 kcal/mol), followed by $\text{lp} \rightarrow \pi^*$ then $\pi \rightarrow \text{lp}^*$. Indeed, the 2A structure of (8,0)-BNNT- NH_3 exhibits more than double the adsorption energy compared to 1A. The similar interaction energies of 1A-1D can be explained on the same character of the acceptor NBOs whether at the edge or the middle. Also, 2B and 2D are isoenergetic ($E_{\text{ad}} = \sim 4.5$ kcal/mol) with 1B or 1D, i.e. middle sites of the tubes. However, it is not clear from NBO interpretation why 2D (near the edge site) behaves differently than the others.

In the BH_3 complexes, BNNTs act as Lewis base, where N atoms are the donor and a vacant p-orbital of BH_3 is the acceptor. In the case of (4,4)-BNNT, BN π NBOs are involved in the interaction, but in the (8,0) counterpart the donor is the N lp at the edge and BN π NBOs at other sites. Since the nature of such NBOs is similar in the armchair tube, either at edge or at the middle, adsorption energies should be in the same range, which is indeed the case in 3B to 3D (~ 7 -8 kcal/mol). Assuming similar contribution in N to B covalent interaction, additional favorable energy of total 20 kcal/mol of 3A comes from 3c-2e bond (**Fig. S10-C**), that is close or may be more than 50% contribution. If that is the case, then 3C ought to exhibit higher adsorption energy than 7 kcal/mol. In this structure, the 3c-2e interaction is weaker than in 3A (based on bond distances), and the participating B atom of the tube is pulled further up above the

surface than the adjacent N atoms, causing some destabilization to reduce the overall interaction energy.

Complex 4A is stabilized by 15 kcal/mol which is reasonable based on the fact that the N lp at the edge is the donor. Except for 4B, the other two structures (4C and 4D) exhibit similar adsorption energy, close to that of 3B-3D, due to the same reason described above. However, the adsorption energy is significantly higher in 4B than 4C or 4D, as this structure is also involved in a 3c-2e bond (**Fig. S10-D**), as in 3A.

Charge redistribution:

To estimate charge redistribution in the most stable BNNT-NH₃/BH₃ structures, atomic charges of BNNT and NH₃/BH₃ were calculated using natural population method^{29, 30}. In addition, total densities of pristine tubes and guest molecules were subtracted from complexes to generate density difference plots, which provide a clear picture of the charge redistribution in the complexes. Such difference plots for the most stable structures are depicted in **Fig. S11** (amount of electron shifts in all cases is tabulated in S12) along with the amount of electron transfer between host and guest.

Since ammonia is donating a lone electron pair (lp) to a vacant p-orbital of boron of the tubes, it is expected that charge will flow from NH₃ to BNNTs. On the other hand in BNNT-BH₃ complexes, charge should flow in the opposite direction, i.e., BNNT will loss electron density, as the active N atom is sharing its lp with B of the guest. Thus, gain or loss by BNNTs will strongly depend on the acid-base character of the guest. Natural group charges clearly support this concept. In 1A and 2A, the Lewis base (NH₃) supplies about 0.33 e to tubes, and the magnitude is independent on the chirality of the tube and the location of NH₃ (see table S12). The amount of electron shift in the simplest Lewis acid-base pair (ammonia-borane) is 0.34 e. These results suggest that the amount of electron flow to the tube may be tunable by changing base character: stronger may add more charge to tubes.

In the case of Lewis acids (BH₃ in the present case), charge should flow from tube to guest, which is true for 4A (**Fig. S11-D**), where a dative covalent interaction is the origin of the stability of the complex. The amount of electron density of 0.30 e is slightly lower than the opposite flow in BNNT-NH₃. It may be noted that this amount is due to a single guest, and in reality BNNTs may host several of them and the cumulative value may be significant.

Interestingly, even for Lewis acid as guest, tubes may gain some electron density provided host-guest interaction includes 3c-2e bonds between them, as in 3A where 0.11 e is transferred to the tube (**Fig. S11-C**). A similar scenario is exhibited by structure 4B (Table S12, not shown in figure), where the amount is 0.14 e. Identifying the source of such reversed trend of electron flow in 3A and 4B complexes is complicated as two dominating factors, B-N dative bond and (H₂)B-H-B(NT) multicenter bond, are involved in the transfer process.

Let us analyze the charge redistribution in diborane to get some idea of the role of the B-H-B 3c-2e bond in 3A and 4B redistribution. In diborane, each boron atom gains 0.5 e at the expense of 0.2 e of each bridging hydrogen and about 0.3e from the other two hydrogens. In structures 3A and 4B, the pertinent B atom of BNNT gains about 0.7 e and the bridging H of BH₃ loses 0.2e, further supporting the similar 3c-2e bond character in these complexes. It appears that this interaction outweighs the transfer of electron from the tube, making it an electron acceptor.

In summary, charge flow from or to BNNT depends on the character of the guest. A Lewis base donates density to the tube, while a Lewis acid accepts electrons from the tube. However, for the latter case multicenter B-H-B bond formation between the tube and Lewis acid reverses the electron flow, making the tube negatively charged. Thus, charge redistribution may be tunable by considering the acid/base strength of any guest molecules, and may facilitate many second functionalization processes, as shown by Sun et al.¹⁷ for CO₂ adsorption.

IR Spectra:

Experimental IR spectra^{41, 42} of pristine BNNTs is dominated by two peaks, one very strong one around 1400 cm⁻¹ (with a shoulder band (medium) around 1350 cm⁻¹) and a weak peak around 800 cm⁻¹. These peaks are assigned as parallel and perpendicular (to the tube axis) BN modes, respectively. Since intensity, predicted by DFT calculations, of parallel BN-modes of both kinds of tubes are very high (8000-14000 km/mol range), theoretical spectra in figures are truncated to 4000 km/mol for clear visibility of weaker peaks.

The parallel BN-mode appears at 1428 cm⁻¹ in pristine (4,4)-BNNT (**Fig. 6A**, red), while the zigzag analogue (**Fig. 6B**, red) exhibits the same mode at a slightly higher frequency (1449 cm⁻¹). Both tubes also show a shoulder peak within 60-90 cm⁻¹ below the sharp and very strong peak. The perpendicular BN-modes of both tubes were found at the same frequency of 759 cm⁻¹, with similar intensity. Thus, theoretical frequencies of pristine tubes are in very good agreement with experimental quantities, indicating solid reliability of the method used.

The next intense and sharp peak appears around 2500 cm⁻¹ in all spectra, in the region of standard B-H stretching modes. For example, the B3LYP/6-31G* frequency of B-H stretching modes of borane is 2614 cm⁻¹, which is in excellent agreement with the experimental value of 2623 cm⁻¹⁴³). The BH stretching frequency of (4,4)-BN tube is 2526 cm⁻¹, while the isoelectronic (8,0) tube exhibits the same mode at 2592 cm⁻¹, i.e., 66 cm⁻¹ higher than armchair counterpart with 1.5 times weaker intensity. Thus, the BH band, in addition to the BN parallel mode, may be used as an indicator to distinguish between the two kinds of tubes. Moreover, the presence of hydrogen at the tips of BN tubes can be identified if a weak but sharp peak is visible near 2500 cm⁻¹. Indeed, some experimental spectra^{41, 44} indicate the presence of a very low peak in that region which is not assigned. Compared to the very strong BN mode, such weak peaks may be difficult to identify or may be overlooked as noise. The intensities of the N-H stretching vibrational modes around 3400 cm⁻¹ (**Fig. 6**) are even lower and unlikely to be detected experimentally. Two other peaks in the 500-1000 cm⁻¹ region arise from BNH or NBH bending vibrations. Intensities of these peaks are close to the BN perpendicular mode of (4,4)-BNNT. However such peaks are less intense in (8,0)-BNNT than (4,4)-BNNT, another difference between these two kinds of tubes.

Near perfect overlap of BN and BH peaks of all complexes (**Fig. 6A-6D**) with those of pristine tubes clearly indicates adsorption of either NH₃ or BH₃ has practically no influence on the IR spectra of BN modes. However, complexes show a few new very weak peaks which may be useful in characterizing different adsorption sites, if those can be detected experimentally. For example, if NH₃ is adsorbed near the edge of (4,4)-BNNT, then two new pure bands at 2395 (B-H stretching) and 1091 (NBH bending) cm⁻¹ in IR spectra of 1D can differentiate from a structure where NH₃ is attached to the middle (1A) of the tube. Both modes are associated with a H-B bond of the tube near the tips where ammonia is adsorbed. The most preferred site of NH₃ at the (8,0)-BNNT surface is also at the edge (2A) and the BH bond should be red-shifted, in

addition to a new peak around 1100 cm^{-1} , due to NBH bending. Indeed, the new peak (green in 8B) at 2474 cm^{-1} , due to pure BH stretching, is red-shifted by about 120 cm^{-1} compared to other B-H modes of BNNTs. Also, a new very weak peak is observed at 1109 cm^{-1} , assigned as a NBH bending frequency.

Since most stable complexes of BNNT-BH₃ (3A and 4B) possess a bridging hydrogen between B of BNNT and B of BH₃, similar to 3c-2e BHB arrangement in diborane, a significant change in the B-H vibrational modes of adsorbent is expected. The bridging B-H bonds of B₂H₆ exhibit a peak at 1663 cm^{-1} , with intensity of 470 km/mol. In both 3A and 4B, a new peak at 1664 (6C, green) and 1653 cm^{-1} (6D, black) further support the presence of a similar bond in BNNTs-BH₃ complexes. However, the intensities of these bands are almost half that of diborane, which may be due to a single B-H-B 3c-2e bond in the complexes instead of two such bonds in B₂H₆.

XPS spectra:

X-ray photoelectron spectroscopy (XPS), also known as electron spectroscopy for chemical analysis (ESCA), is extensively used for the characterization of pristine and chemically modified BNNTs. The experimental binding energies of B 1s and N 1s of pristine BNNTs are ~ 190.0 and $\sim 398.0\text{ eV}$ ^{41,45}, respectively, and these energies may be considered as standard BEs for pristine BNNTs. Chemical modification changes these values depend on the functional groups and how they are chemically linked to either B or N atoms at the surface.

In the simulation of XPS binding energies, core orbital energies were obtained from natural bond orbital (NBO) analysis, and the negative of core orbital energy (Koopman's theorem⁴⁶) is used to estimate 1s binding energy. However, it is worth mentioning that the BEs from theoretical simulation may differ from experimental data due to level of theory and non-adiabatic assumption, and requires a scale factor for better correlation with experimental results. For example, a recent theoretical study⁴⁷ of several carbon-based organic molecules proposed a scale factor for C 1s. However, no comparable study on simulation of BNNTs, to our knowledge, has been reported yet and to establish a scale factor for B and N 1s BEs several tubes have to be considered in the test bed, which is not the target of the present study. Since we are interested in the changes in BEs of B 1s and N 1s upon complexation, not the absolute values, these energies from NBO calculations may be used comfortably.

Binding energies of B 1s and N 1s of BNNTs and NH₃/BH₃ and their shifts in complexes are summarized in Table 2. To estimate the changes in 1s orbital energy of B and N atoms of the tubes, 1s energy of those atoms directly bonded to ammonia or borane molecules were subtracted from the 1s energy of the same atoms of the pristine tubes. Due to different chemical environment near the tips and middle of the tubes, BEs are slightly different, as shown in the first two rows of the table. The B 1s and N 1s binding energies of ~ 181.5 and $\sim 384.0\text{ eV}$ are respectively lower by about 9.0 and 14.0 eV than experimental values. The dative covalent bond formation between ammonia and borane molecules changes the BEs considerably: the B 1s energy decreases by 2.7 eV from 182.0 eV of BH₃, while the N core orbital gains 2.5 eV from isolated ammonia. Similar changes are expected for BNNT-NH₃/BH₃ complexes if components behave as Lewis acid and base, similar to ammonia borane.

Indeed, the change in core orbital energy of adsorbates in complexes follows the same trends where interaction with tube solely involves N→B dative bond. For example, the magnitude of Δ_{BE} of N (NH₃) 1s in 1A, 1D and 2A (+2.34, +2.49 and +2.43 eV, respectively) are

very close to +2.50 eV in ammonia borane. In 4A, where BH_3 is linked to one of the N atoms near the tip of (8,0)-BNNT via a dative bond, the B 1s energy of borane is lowered from -2.70 eV to -2.44 eV. In other cases (3A and 4B), the bonding situation is different than in 4A, where one of the B-H bonds is involved in 3c-2e bond in addition to the dative bond. This combination of two favorable interactions seems unique and change (less than half of 4A) in the B (BH_3) 1s energy may be an indicator of such structural arrangement.

The shift of about +1.0 eV in BE 1s of active N of BNNTs (3A, 4A and 4B) is less than half of that of N of NH_3 and such change is almost independent on the chirality of tubes and multi-center bond formation by attached BH_3 molecule. On the contrary, the shifts in 1s energy of B of BNNTs in 1A, 1D and in 2A complexes are negligible and can be in either positive or negative direction, depending on the position of active N atom. If the adsorption site is at the tips (B of the tube is attached to a hydrogen and two nitrogen atoms), BE is lowered by 0.04 in 1D and 0.23 in 2A tubes, otherwise the shift is positive (+0.31 eV in 1A). Such changes may be generalized as shift in 2B (+0.30 eV) and 2C (+0.32 eV) (not shown), where NH_3 is bonded to B atom at the middle, also follows the same trends.

NMR data:

We also calculated NMR spectra, which is equally useful as other analytical tools in the characterization of a wide range of compounds and materials. However, NMR studies on BNNTs are meager and our present findings may elevate the importance and interest of using such analytical tools for understanding structures of chemically modified BNNTs. In Table 3, calculated values of isotropic shielding constant (σ_{iso}) of ^{11}B and ^{15}N of tubes and guest molecules, and their chemical shifts (δ) upon complexation are summarized.

Since both B and N atoms of the tubes are in different chemical environments (at the tips and at the middle of the surface), they are expected to experience different shielding. Tabulated data indeed show differences in σ_{iso} of ^{11}B and ^{15}N of tubes. In the present context, we are more interested in chemical shifts, in reference to pristine tube and guest molecules that may be observable in experimental NMR spectra. As in XPS spectra, the δ values of atoms of BNNTs directly involved in dative bond with guest molecules are presented in the table.

Our reference molecule $\text{H}_3\text{N-BH}_3$ exhibits a significant downfield shift of 103 ppm in δ of ^{11}B , while that of ^{15}N showed opposite sign and one-fourth its magnitude. Such a large shift in ^{11}B is found in several boron compounds⁴⁸. These changes in δ values are due to change in sp^2 to sp^3 hybridization of B and change from tri-coordination to tetra-coordination of N atom in ammonia borane. Changes in chemical shifts in complexes are expected to follow similar trends, but their magnitude in BN tubes may vary because of different chemical environments.

Indeed, ammonia-BNNT complexes (1A, 1D and 2A) follow the same trend, but the magnitude of chemical shift of ^{15}N is close to double that of $\text{H}_3\text{N-BH}_3$. Changes in chemical shift of ^{11}B of BH_3 are in the range of 26-35 ppm, about 3.5 times smaller than ammonia-borane. When BH_3 is adsorbed at the surface of BNNTs, almost no change is found in the chemical shift of ^{11}B . But the active nitrogen of 3A, 4A and 4B shows a down-shift in δ , i.e., a reverse trend compared to NH_3 . The magnitude of such a shift strongly depends on whether a 3c-2e bond is present. In absence of such a bond as in 4A, δ of N is +24 ppm, but it increases to +81 ppm in 3A and to +90 ppm in 4B, where a B-H-B 3c-2e bond is present.

The chemical shift of the bridging hydrogen of B-H-B 3c-2e bond in 3A and 3B may provide some additional data for identification. In the case of diborane, δ of the bridging proton

is +9 ppm in reference to BH_3 . Complexes 3A and 4B also exhibit similar values (about +7 ppm) in support of such bonds.

In summary, Lewis acid-base complex formation between BNNTs and NH_3/BH_3 causes significant changes in XPS spectra and chemical shift of atoms directly involved in such interactions. Such changes may be valuable in characterization of complex structures.

Interactions with other acids:

Results from the above sections clearly indicate BNNTs can act as Lewis base as well as acid, and the strength of the interaction varies from 3-20 kcal/mol depending on the location of the acid/base centers on the tube and chirality of the tube. Natural curiosity arises as to how such interactions might change with other guest acids and bases. In order to examine such effects, neutral AlH_3 , BF_3 , BCl_3 , BH_2CH_3 and an ionic CH_3^+ were allowed to interact at the edge (e) and middle (m) base sites of BNNTs, as these two sites were found most active. Geometries were fully optimized at the B3LYP/6-31+G* level and interaction energies were again corrected for basis set superposition errors. Optimized geometries of the most stable neutral acid-BNNT adducts are summarized in **Fig. 7** and other less stable structures in **Fig. S13-S16**. For the sake of comparison, results from the interaction of these acids with NH_3 are also shown in all figures. Table 4 displays counterpoise corrected interaction energies of this series of adducts, and the effect of BSSE on such energies (1-3 kcal/mol) can be obtained from Table S17.

Replacing BH_3 by AlH_3 seems to have little effect on the interaction energies at both interaction sites (edge and middle) in both kind of tubes. For example, when attached at the edge N-site, complexation energies are 20.0 kcal/mol for BH_3 and 19.0 for AlH_3 . Similarly, interaction energies at other sites are also comparable. Like $\text{BH}_3\text{-NH}_3$, the interaction between AlH_3 with ammonia is also slightly stronger (26.0 kcal/mol) than the most stable (4,4)-BN- $\text{AlH}_3(\text{e})$ structure. Similar to (4,4)BNNT- BH_3 (3A), the most stable (4,4)-BN- $\text{AlH}_3(\text{e})$ also exhibits a 3c-2e Al-H-B(NT) bond which is responsible for added stability in comparison to other structures. The Al-N(NT) distances, except for the most stable structure, are slightly longer than in simpler complex structures. From the energetic perspective, AlH_3 prefers the edge site of both tubes over the middle site, and the preference for the (4,4) tube is slightly greater (by 4.0 kcal/mol) than in the (8,0) tube. In (4,4)-BN- $\text{AlH}_3(\text{e})$, AlH_3 donates 0.48 e to the tube and this amount is more than four times that in BH_3 complex (3A). Similar to BH_3 , AlH_3 in other locations accepts electrons from the tube (**Fig. 7** and S13) but in lesser amounts.

BF_3 on the edge of (8,0)-BNNT(e) forms a stable complex with an interaction energy of 6.9 kcal/mol (**Fig. 7**), whereas all other structures exhibit an adsorption energy of about 1.0 kcal/mol or less (**Fig. S14**). Exchange of all F atoms by Cl makes structures unstable by 2-14 kcal/mol (**Fig. S15**) except (8,0)BN- $\text{BCl}_3(\text{e})$ (**Fig. 7**) where the interaction is weaker than BF_3 by 2.3 kcal/mol. Thus, the presence of electron rich and highly electronegative groups in guest BR_3 acid hinders the base character of BNNTs. This may be due to steric effect and strong repulsion between electron-rich F and N of tubes that outweigh the attractive covalent interaction. Electron transfer from the tube in the stable adducts of BF_3 and BCl_3 follows the same trend as in BH_3 .

Substitution of a hydrogen of BH_3 by electron-donating methyl group causes favorable interaction at the edge only. Placing BH_2CH_3 at the middle of the tube did not result in an

optimized structure for either sort of tube. The most stable (8,0)BN-BH₂CH₃(e) structure (Fig. 7) is stabilized by 6.2 kcal/mol. Thus, derivatives of borane form a weaker complex with BNNTs, and are selectively attached to the edges of the (8,0)BN tube. About 0.29 e flows from tube to the adsorbate in the most stable structure.

Strongest interactions with BNNTs are found with ionic acid group. In Fig. 8, results of BNNTs-CH₃⁺ are summarized along with structure and complexation energy between NH₃ and CH₃⁺. Whether with ammonia or BNNTs, the interaction energy is more than 100 kcal/mol, irrespective of tube chirality or the adsorption sites. The strongest interaction (114 kcal/mol) is found in (8,0)BN-CH₃⁺ (e). This quantity surpasses the interaction between ammonia and methyl ion by about 4 kcal/mol. In all complexes, the cation is partially neutralized by the transfer of about 0.7 e from the tube.

In summary, Lewis acids containing a metal atom may form a stronger adduct with BNNTs and would prefer the edge over middle sites; however, the latter sites are also favorable. Ionic acids most likely form strongly bonded complexes in any site and independent of chirality of the BN-tube. Electron-rich acids may selectively attach to the edge of zigzag BNNTs, rather than analogous armchair BN tubes. This may be due to dominating electrostatic repulsion between electron-rich guest acids and electron-rich nitrogen atoms of BN-tubes.

Interactions with other bases:

Although there has been active research on amine-functionalized BNNTs for several years^{18-20, 49-52} the location of the amine group at the surface of each tube is still not known. Since previous theoretical investigations used periodic boundary condition (PBC) model by considering amine groups at the middle of the tube surface, the interaction at the edge of the tube remains unexplored. In the present study, we found the preference of NH₃ depends on the location of acidic B-sites as well as the chirality of the BN-tube. To strengthen our findings, we added results of methyl-amine (CH₃NH₂) interacting on the surface of the tube. Same strategies of active acid B-sites and methods, as described for ammonia cases, were employed here. Optimized geometries, interaction energies, along with charge transfer between host-guest, are summarized in Fig. 9 and energetic information is listed in Table 4.

Similar to NH₃-(4,4)BNNT, methylamine has little preference for edge vs middle site; complexation energy of about 6.6 kcal/mol is higher by about 2 kcal/mol than in ammonia complexes (Fig. 1). Also, the amine group prefers (8,0)BN tube over its related armchair tube, and adsorption at the edge stabilizes the complex by 11.5 kcal/mol, the same as that of ammonia complex 2A. The middle site of both tubes accommodates the amine at the same energy (about 7 kcal/mol). Although the reaction between borane with methylamine stabilized the complex by 32.4 kcal/mol, the amount of electron transfer from amine to tube (~0.33 e) is the same for all cases. In all cases, tubes gain about 0.3 e from the base and this quantity is independent of the strength of interaction.

The next amino functional groups considered is NH₂COOH and results are summarized in Fig. 10 and in Table 4. None of the stable complexes show N→B dative covalent bond as in all other cases discussed above. The most stable (8,0)-NH₂COOH (e) and (4,4)-NH₂COOH (e) exhibit O--H-N(NT) and N-H--N(NT) hydrogen bonds. The former structure is stabilized by 7.8 kcal/mol, whereas the interaction energy in the latter armchair structure is almost half that. It may be noted that the same N atoms of tube participate in those H-bonds. Other structures, where a single O-H--N(NT) bond is the means of interaction at the middle of the tube surface, is

stabilized by about 2-3 kcal/mol. When the single NH bond of NH_2COOH is linked to N of the tube, the H-bond energy reduces to 0.9 kcal/mol. Stronger H-bonds are associated with shorter distance - this rule is also obeyed in the present cases. These results are in accordance with standard H-bond theory⁵³. Amino acids contain both NH_2 and COOH groups and are expected to undergo similar H-bond formation at the surface of BNNTs, where N atoms of tube act as proton acceptor. Nitrogen atoms at the edge may show dual character – proton donor as well as proton acceptor. Recently, sensitivity of BNNTs towards aromatic amino acids has been reported by Mukhopadhyay et al.⁵⁴ who found a polar biomolecule interacts more strongly at the surface of the tube than non-polar molecules.

Conclusions:

Lewis acid and base character of single-wall boron nitride nanotubes and the fundamentals of interactions (such as interaction energy, charge redistribution and their IR, NMR, XPS spectral characterizations) with different guest acids and bases at the N and B sites of BNNTs have been explored using DFT theory. Due to the examination of electron-rich N atoms, inclusion of diffuse sp functions (such as 6-31+G* basis set) seems appropriate for the description of such interactions. Results from this study recommend considering counterpoise correction (due to basis set superposition error) to interaction energies. However, no significant changes have been noted in geometric parameters due to such corrections.

The strength of these interactions depends on the locations of the acidic and basic sites of the BN-tubes and also on the chirality of the tubes. Furthermore, the character of the adsorbates also plays a significant role in selecting sites of the tube. For example, interaction with ionic CH_3^+ acid is very strong (more than 100 kcal/mol), and imparts positive charge to the tube. While NH_3 prefers zigzag over armchair tube, BH_3 opts for both with slight preference for the latter kind of tube. The presence of electron-rich elements in guest acids (such as BF_3 and BCl_3), weakens the interaction from 15-20 kcal/mol in BH_3 to a few kcal/mol, due to electrostatic repulsion between F or Cl atoms with N atoms of tube. Preference and strength of interaction between AlH_3 and BNNT followed the same trends as found in BH_3 , which indicates guest acid with a metal atom will interact strongly with the tube

In general, BNNT tubes donate electrons to acids while a reverse trend follows for interacting bases. Some of the adducts gained extra stability due to the formation of 3c-2e bonds with BH_3 and AlH_3 , which reversed the electron flow making tubes negatively charged. In all cases studied, covalent B-N bond formation is responsible for the stability of the complex, in addition to multi-center bonding with electron-deficient BH_3 and AlH_3 . However, when the guest molecule contains both amine and carboxylic groups, as in NH_2COOH , hydrogen bonding plays a significant role in stability of the resulting complexes.

In most complexes, edge sites are found more favorable than middle sites, both for guest acids or bases. Such preference for edge sites can be rationalized from NBO analyses and geometric parameters, such as tetrahedral angles of active sites. Since modeling edge functionalization is not possible in periodic boundary approach, alternate molecular models are the only alternative to study such interactions.

IR spectra of ammonia-BNNTs and borane-BNNTs exhibit some new characteristic features that can be used to identify complexation and to some extent location of reacting acid and base. However, such characteristic peaks are extremely weak compared to the B-N modes, and may need special techniques to observe them. Simulation of XPS and NMR spectra of the

complexes revealed significant changes from the pristine tube as well as the guest acids or base, and should be observable in experimental spectra.

These findings may help in selective functionalization of smaller diameter BNNTs using a wide range of compounds, having acidic or basic centers or both. Since edges are more active, BNNT has potential application as AFM tips, besides complex formations that may have other applications such as (bio)sensors and composite materials. The zigzag tube has another advantage over armchair tube because it contains B-rich and N-rich tips (scheme I) which may be utilized simultaneously as acid-base centers.

Acknowledgements: One of the authors (S. Rajashabala) wishes to thank University Grants Commission (UGC) of India for providing financial support to carry out research in the USA under Indo-US Raman Post-Doctoral Fellowship Program. DoD HPC center and HPC center at Utah State University are acknowledged for providing computational facilities.

Figure Captions:

Fig. 1. BSSE corrected B3LYP/6-31+G* optimized structures of (4, 4)-BNNT-NH₃. Blue, yellow and grey colors represent N, B and H atoms, respectively. Bond lengths are in Å. Where BN bond distances are same in the vicinity of the active site, only one of those distances is shown.

Fig. 2. BSSE corrected B3LYP/6-31+G* optimized structures of (8, 0)-BNNT-NH₃. Blue, yellow and grey colors represent N, B and H atoms, respectively. Bond lengths are in Å. Where BN bond distances are same in the vicinity of the active site, only one of those distances is shown.

Fig. 3. BSSE corrected B3LYP/6-31+G* optimized structures of (4, 4)-BNNT-BH₃. Blue, yellow and grey colors represent N, B and H atoms, respectively. Bond lengths are in Å. Where BN bond distances are same in the vicinity of the active site, only one of those distances is shown.

Fig. 4. BSSE corrected B3LYP/6-31+G* optimized structures of (8,0)-BNNT-BH₃. Blue, yellow and grey colors represent N, B and H atoms, respectively. Bond lengths are in Å. Where BN bond distances are same in the vicinity of the active site, only one of those distances is shown.

Fig. 5. Natural bond orbitals (NBO) of pristine BNNTs and lone pair of NH₃ and vacant π NBO of BH₃. lp stands for lone pair, and * indicates antibonding/vacant NBOs.

Fig. 6. IR spectra of most stable BNNT-NH₃/BH₃. Lorentzian broadening with fwhm of 20 cm⁻¹ was applied to each spectrum.

Fig. 7. B3LYP/6-31+G* optimized structures of H₃N-AlH₃/BF₃/BCl₃/BH₂CH₃ and corresponding BNNT-AlH₃/BF₃/BCl₃/BH₂CH₃. Bond lengths are in Å and angles are in degree. e and m stand for edge and middle adsorption sites of the tube, respectively. BSSE corrected adsorption energies (in kcal/mol) are given in bold and a positive value indicates attractive interaction between two units, otherwise interaction is repulsive. Most stable structures are shown in this figure and other structures are given in **Fig. S13-S16**. Electron transfer from or to BNNTs are shown by arrow with number of electron.

Fig. 8. B3LYP/6-31+G* optimized structures of H₃N-CH₃⁺ and BNNT-CH₃⁺. Bond lengths are in Å and angles are in degree. e and m stand for edge and middle adsorption sites of the tube, respectively. BSSE corrected adsorption energies (in kcal/mol) are given in bold and a positive value indicates attractive interaction among between two units. Electron transfer from or to BNNTs are shown by arrow with number of electron.

Fig. 9. B3LYP/6-31+G* optimized structures of H₃B-NH₂CH₃ and BN-NH₂CH₃. Bond lengths are in Å and angles are in degree. e and m stand for edge and middle adsorption sites of the tube, respectively. BSSE corrected adsorption energies (in kcal/mol) are given in bold and a positive

value indicates attractive interaction among between two units, otherwise interaction is repulsive. Electron transfer from or to BNNTs are shown by arrow with number of electron.

Fig. 10. B3LYP/6-31+G* optimized structures of BN-NH₂COOH. Bond lengths are in Å and angles are in degree. BSSE corrected adsorption energies (in kcal/mol) are given in bold and a positive value indicates attractive interaction among between two units, otherwise interaction is repulsive

Supporting Information:

Effect of basis sets on adsorption energies (S1) and geometric parameters (S2-S3), effect of tube length and diameter (S4, S5), hybridization angles (S6-S9), NBOs of complexes (S10), density difference plots and electron shift from/to BNNTs (S11, S12), optimized structures, electron flow from/to BNNTs and adsorption energies of other acids (AlH₃, BF₃, BCl₃ and BH₂CH₃ (S13-S17)).

REFERENCES

1. G. N. Lewis, *Valence and the structure of atoms and molecules*, The Chemical Catalog Co, Inc., New York, 1923.
2. A. Rubio, J. L. Corkill and M. L. Cohen, *Phys. Rev. B*, 1994, **49**, 5081-5084.
3. X. Blase, A. Rubio, S. G. Louie and M. L. Cohen, *Europhys. Lett.*, 1994, **28**, 335-340.
4. N. G. Chopra, R. J. Luyken, K. Cherrey, V. H. Crespi, M. L. Cohen, S. G. Louie and A. Zettl, *Science*, 1995, **269**, 966-967.
5. M. Terrones, W. K. Hsu, H. Terrones, J. P. Zhang, S. Ramos, J. P. Hare, R. Castillo, K. Prasside, A. K. Cheetham, H. W. Kroto and D. R. M. Walton, *Chem. Phys. Lett.*, 1996, **259**, 568-573.
6. A. Loiseau, F. Willaime, N. Demoncy, G. Hug and H. Pascard, *Phys. Rev. Lett.*, 1996, **76**, 4737-4740.
7. M. Terauchi, M. Tanaka, M. Takehisa and Y. Saito, *J. Electron Microsc.*, 1998, **47**, 319-324.
8. D. Golberg, Y. Bando, M. Eremets, K. Takemura, K. Kurashima, K. Tamiya and H. Yusa, *Chem. Phys. Lett.*, 1997, **279**, 191-196.
9. T. Laude, Y. Matsui, A. Marraud and B. Jouffrey, *App. Phys. Lett.*, 2000, **76**, 3239-3241.
10. D. Golberg, Y. Bando, T. Sato, N. Grobert, M. Reyes-Reyes, H. Terrones and M. Terrones, *J. Chem. Phys.*, 2002, **116**, 8523-8532.
11. S. Iijima, *Nature*, 1991, **354**, 56-58.
12. S. Iijima and T. Ichihashi, *Science*, 1993, **363**, 603-605.
13. J. Garel, L. I., C. Zhi, K. S. Nagapriya, R. Popovitz, D. Golberg, Y. Bando, O. Hod and E. Joselevich, *Nano Lett.*, 2012, **12**, 6347-6352.
14. Huang, J. Lin, J. Zou, M.-S. Wang, K. Faerstein, C. Tang, Y. Bando and D. Golberg, *Nanoscale*, 2013, **5**, 4840-4846.

15. D. Golberg, Y. Bando, Y. Huang, T. Terao, M. Mitome, C. Tang and C. Zhi, *ACS Nano*, 2010, **4**, 2979-2993.
16. C. Zhi, Y. Bando, C. Tan and D. Golberg, *Solid State Commun.*, 2005, **135**, 67-70.
17. Q. Sun, Z. Li, D. J. Searles, Y. Chen, G. Lu and A. Du, *J. Am. Chem. Soc.*, 2013, **135**, 8246-8253.
18. S. Pal, S. R. C. Vivekchand, A. Govindaraj and C. N. R. Rao, *J. Mater. Chem.*, 2007, **17**, 450-452.
19. A. Maguer, E. Leroy, L. Bresson, E. Doris, A. Loiseau and C. Mioskowski, *J. Mater. Chem.*, 2009, **19**, 1271-1275.
20. X. Wu, W. An and X. C. Zeng, *J. Am. Chem. Soc.*, 2006, **128**, 12001-12006.
21. Y. Li, Z. Zhou and J. Zhao, *J. Chem. Phys.*, 2007, **127**, 184705-184706.
22. A. Ahmadi, J. Beheshtian and N. L. Hadipour, *Struct. Chem.*, 2011, **22**, 183-188.
23. E. Zahedi, *Physica B*, 2012, **407**, 3841-3848.
24. A. Rimola and M. Sodupe, *Phys. Chem. Chem. Phys.*, 2013, **15**, 13190-13198.
25. A. D. Becke, *J. Chem. Phys.*, 1993, **98**, 5648-5652.
26. C. Lee, W. Yang and R. G. Parr, *Phys. Rev. B*, 1988, **37**, 785-789.
27. S. F. Boys and F. Bernardi, *Mol. Phys.*, 1970, **19**, 553-566.
28. R. D. Johnson III, NIST computational chemistry comparison and benchmark database. 2006. Available from: <http://cccbdb.nist.gov/>.
29. A. E. Reed, F. Weinhold, L. A. Curtiss and D. J. Pochatko, *J. Chem. Phys.*, 1986, **84**, 5687-5705.
30. A. E. Reed, L. A. Curtiss and F. Weinhold, *Chem. Rev.*, 1988, **88**, 899-926.
31. K. Wolinski, J. F. Hilton and P. Pulay, *J. Am. Chem. Soc.*, 1991, **112**, 8251-8260.
32. J. R. Cheeseman, G. W. Trucks, T. A. Keith and M. J. Frisch, *J. Chem. Phys.*, 1996, **104**, 5497-5509.
33. M. J. Frisch, G. W. Trucks, H. B. Schlegel, G. E. Scuseria, M. A. Robb, J. R. Cheeseman, G. Scalmani, V. Barone, B. Mennucci, G. A. Petersson, H. Nakatsuji, M. Caricato, X. Li, H. P. Hratchian, A. F. Izmaylov, J. Bloino, G. Zheng, J. L. Sonnenberg, M. Hada, M. Ehara, K. Toyota, R. Fukuda, J. Hasegawa, M. Ishida, T. Nakajima, Y. Honda, O. Kitao, H. Nakai, T. Vreven, J. Montgomery, J. A., J. E. Peralta, F. Ogliaro, M. Bearpark, J. J. Heyd, E. Brothers, K. N. Kudin, R. Kobayashi, J. Normand, K. Raghavachari, A. Rendell, J. C. Burant, S. S. Iyengar, J. Tomasi, M. Cossi, N. Rega, N. J. Millam, M. Klene, J. E. Knox, J. B. Cross, V. Bakken, J. Jaramillo, R. E. Stratmann, O. Yazyev, A. Austin, C. Pomelli, J. W. Ochterski, R. L. Martin, K. Morokuma, V. G. Zakrzewski, G. A. Voth, P. Salvador, J. J. Dannenberg, S. Dapprich, A. D. Daniels, Ö. Farkas, J. B. Foresman, J. V. Ortiz, J. Cioslowski and D. J. Fox, *Gaussian09*, Gaussian, Inc., Wallingford CT, USA, 2009.
34. G. A. Zhurko, <http://www.Chemcraftprog.Com>.
35. A. B. Sannigrahi and T. Kar, *Chem. Phys. Lett.*, 1990, **173**, 569-572.
36. V. Joans, G. Frenking and M. T. Reetz, *J. Am. Chem. Soc.*, 1994, **116**, 8741-8753.
37. T. Kar and S. Scheiner, *J. Chem. Phys.*, 2003, **119**, 1473-1482.
38. J. D. Carpenter and B. S. Ault, *Chem. Phys. Lett.*, 1992, **197**, 171-174.
39. S. Saha, T. C. Dinadayalane, D. Leszczynski and J. Leszczynski, *Chem. Phys. Lett.*, 2013, **565**, 69-73.

40. E. L. Muetterties, ed., *Boron hydride chemistry*, Academic Press Inc, Massachusetts, 1975.
41. C. Y. Zhi, Y. Bando, T. Terao, C. C. Tang, H. Kuwahara and D. Golberg, *Chem. Asian J.*, 2009, **4**, 1536-1540.
42. Z. Dong and Y. Song, *J. Phys. Chem. C*, 2010, **114**, 1782-1788.
43. W. J. Hehre, L. Radom, P. v. R. Schleyer and J. A. Pople, *Ab Initio Molecular Orbital Theory*, Willey & Sons, New York, 1986.
44. S. Kalay, Z. Yilmaz and M. Culha, *Beilstein J. Nanotechnol.*, 2013, **4**, 843-851.
45. C.-Y. Su, Z.-Y. Juang, K.-F. Chen, B.-M. Cheng, G.-R. Chen, K.-C. Leou and C.-H. Tsai, *J. Phys. Chem. C*, 2009, **113**, 14681-14688.
46. T. Koopman, *Physica*, 1934, **1**, 104-113.
47. M. Giesbers, A. T. M. Marcelis and H. Zuilhof, *Langmuir*, 2013, **29**, 4782-4788.
48. S. Hermanek, *Chem. Rev.*, 1992, **92**, 325-362.
49. T. Ikuno, T. Sainsbury, D. Okawa, J. M. J. Frechet and A. Zettl, *Solid State Commun.*, 2007, **142**, 643-646.
50. T. Sainsbury, T. Ikuno, D. Okawa, D. Pacile, J. M. J. Frechet and A. Zettl, *J. Phys. Chem. C*, 2007, **111**, 12992-12999.
51. E. C. Anota, A. R. Juarez, M. Castro and H. H. Coccoletzi, *J. Mol. Model*, 2013, **19**, 321-328.
52. A. A. Peyghan and Z. Bagheri, *Acta Chim. Slov.*, 2013, **60**, 743-749.
53. S. Scheiner, *Hydrogen Bonding. A Theoretical Perspective*, Oxford University Press, Oxford, 1997.
54. S. Mukhopadhyay, R. H. Scheicher, R. Pandey and S. P. Karmna, *J. Phys. Chem. Lett.*, 2011, **2**, 2442-2447.

Table 1. B3LYP/6-31+G* adsorption energies (E_{ad}), BSSE corrected adsorption energies ($E_{ad(CP)}$) and deformation energies (E_{Def}) of BNNT-NH₃ and BNNT-BH₃ (see Figs. 1-4 for structures). All energies are in kcal/mol.

	E_{ad}	$E_{ad(CP)}$	E_{Def} BN tube	E_{Def} NH ₃ /BH ₃
(4,4)-BNNT-NH₃				
1A	7.58	4.58	18.80	0.09
1B	7.64	4.84	18.83	0.09
1C	7.49	4.49	18.20	0.08
1D	7.20	4.60	18.88	0.08
(8,0)-BNNT-NH₃				
2A	14.03	11.44	19.46	0.09
2B	7.68	4.72	19.43	0.10
2C	7.28	4.28	19.54	0.13
2D	1.29	-1.43	16.59	0.06
(4,4)-BNNT-BH₃				
3A	21.05	19.96	21.06	26.84
3B	9.28	8.28	3.68	11.01
3C	8.39	7.19	17.12	22.85
3D	7.85	6.78	3.04	10.44
(8,0)-BNNT-BH₃				
4A	15.80	14.69	3.74	12.08
4B	15.53	14.47	19.24	25.30
4C	8.04	6.99	3.30	11.16
4D	7.71	6.59	3.29	12.01

Table 2. Binding energies (BE, in eV) of 1s core electron of B and N atoms and their changes (Δ_{BE} in eV) in ammonia-borane and complexes with respect to NH_3/BH_3 and pristine tube.

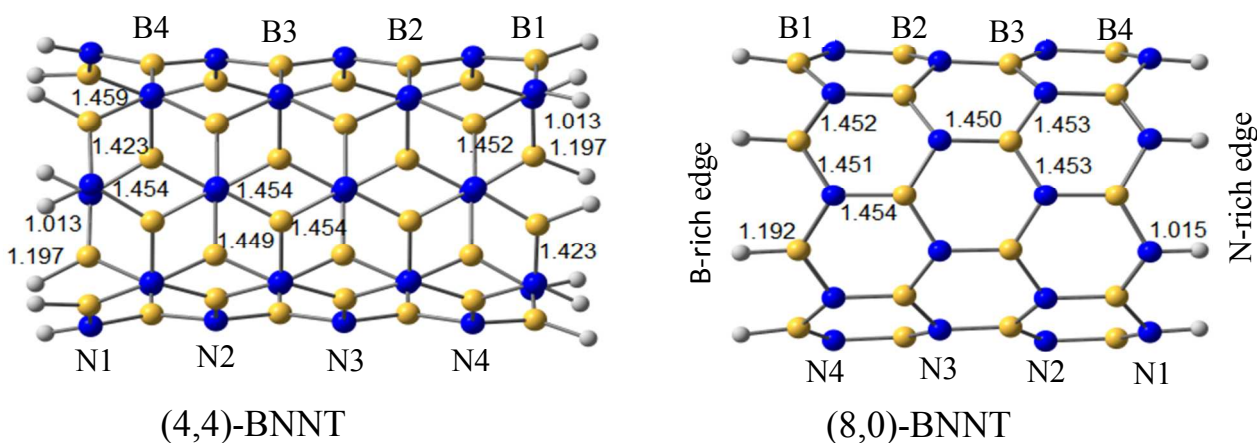
System	BE	BE
(4,4)-BNNT	181.5 - 181.9	384.5 - 383.3
(8,0)-BNNT	181.53 - 181.8	383.32- 384.5
$\text{BH}_3 / \text{NH}_3$	182.0	385.6
	Δ_{BE} (B 1s)	Δ_{BE} (N 1s)
$\text{H}_3\text{B-NH}_3$	-2.70	+2.50
	B(BNNT)	N(NH_3)
1A (4,4)-BNNT- NH_3	+0.31	+2.34
1D (4,4)-BNNT- NH_3	-0.04	+2.49
2A (8,0)-BNNT- NH_3	-0.23	+2.43
	B(BH_3)	N(BNNT)
3A (4,4)-BNNT- BH_3	-1.08	+1.04
4A (8,0)-BNNT- BH_3	-2.44	+1.01
4B (8,0)-BNNT- BH_3	-1.09	+0.97

Table 3. Chemical isotropic shielding (σ_{iso} in ppm) of B and N atoms of BNNTs and NH_3/BH_3 , and their chemical Shift (δ , in ppm) in $\text{H}_3\text{B-NH}_3$ and complexes (relative to isolated NH_3/BH_3 and pristine tubes).

System	σ_{iso}	σ_{iso}
(4,4)-BNNT	79.96 - 83.8	134.2 - 146.0
(8,0)-BNNT	75.73 - 84.4	109.54 - 168.6
$\text{BH}_3 / \text{NH}_3$	27.69	254.98
	δ ^{11}B	δ ^{15}N
$\text{H}_3\text{B-NH}_3$	+103	-24
	B(BNNT)	N(NH_3)
1A (4,4)-BNNT- NH_3	+26	-47
1D (4,4)-BNNT- NH_3	+33	-44
2A (8,0)-BNNT- NH_3	+35	-39
	B(BH_3)	N(BNNT)
3A (4,4)-BNNT- BH_3	+103	+81
4A (8,0)-BNNT- BH_3	+95	+24
4B (8,0)-BNNT- BH_3	+101	+90

Table 4. BSSE corrected B3LYP/6-31+G* adsorption energies ($E_{ad(CP)}$). e and m stand for the edge and middle site of the tube, respectively. All energies are in kcal/mol, and positive value means attractive interaction, otherwise repulsive. Structures are shown in Figs. 7-10 and S13-S16.

	BNNT as Lewis Base (LB)		NH ₃ as LB
	(4,4)	(8,0)	
Lewis acids	$E_{ad(CP)}$	$E_{ad(CP)}$	$E_{ad(CP)}$
BH ₃ (e)	20.0 (3A)	14.7 (4A)	28.3
BH ₃ (m)	8.3 (3B)	7.0 (4C)	
AlH ₃ (e)	19.0	15.1	26.0
AlH ₃ (m)	8.9	8.1	
BF ₃ (e)	1.0	6.9	20.7
BF ₃ (m)	1.1	0.6	
BCl ₃ (e)	-2.4	4.6	21.2
BCl ₃ (m)	-13.1	-14.4	
BH ₂ CH ₃ (e)	1.4	6.2	21.3
CH ₃ ⁺ (e)	109.2	113.8	109.8
CH ₃ ⁺ (m)	110.6	107.3	
Lewis bases	BNNT as Lewis Acid (LA)		BH ₃ as LA
NH ₃ (e)	4.6	11.4	28.3
NH ₃ (m)	4.6	4.7	
NH ₂ CH ₃ (e)	6.6	11.5	32.4
NH ₂ CH ₃ (m)	6.7	7.1	
NH ₂ COOH			12.2
H-Bond			
NH ₂ COOH (e)	4.1	7.8	11.2
NH ₂ COOH (m)	2.8	2.0	
NH ₂ COOH (m1)		0.9	



Scheme I. B3LYP/6-31+G* (counter-poise corrected) structures and geometric parameters (in Å). Possible Lewis acid centers (B1-B4) and Lewis base centers (N1-N4) of both tubes are shown, where B1 and N1 centers are at the edge, B4/N4 is near the edge and rest are at the middle of the tube surface. The difference between edge and near-edge is the environment; in the former B/N is bonded to two N atoms and one terminating H atom, while later centers are surrounded to three N or B atoms.

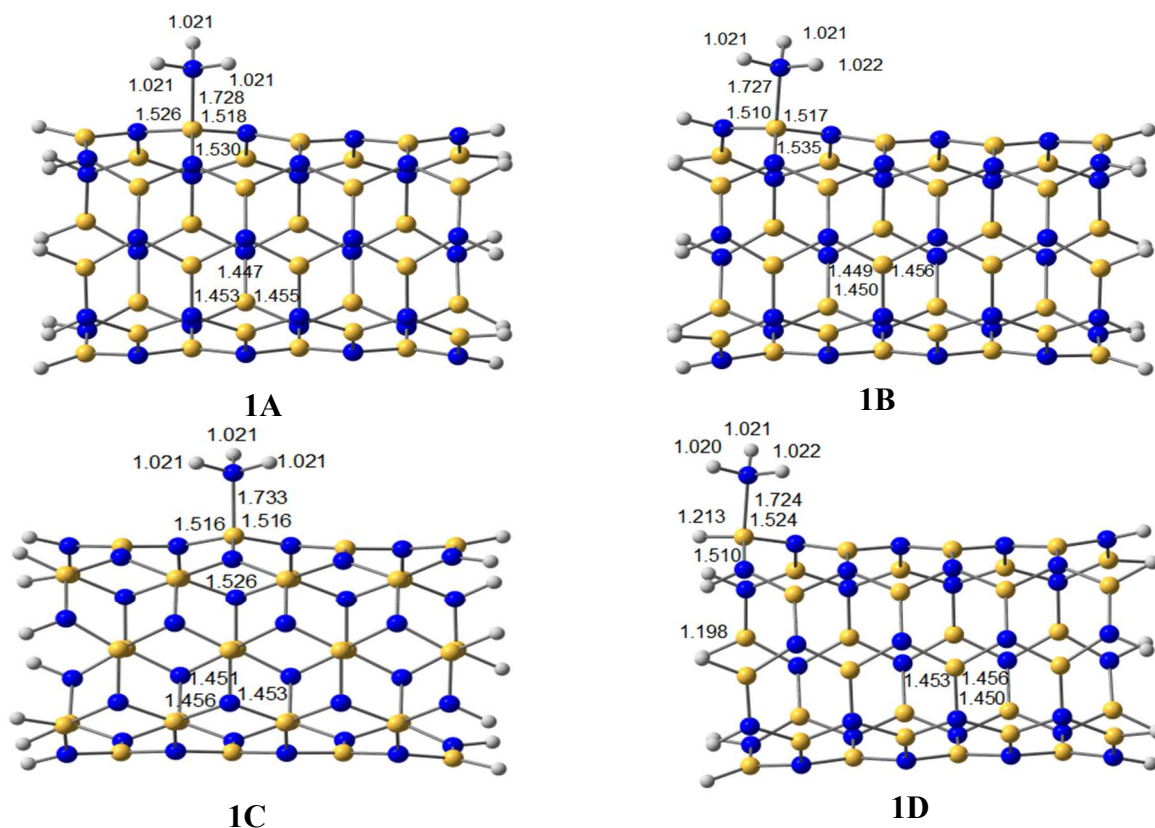


Fig. 1. BSSE corrected B3LYP/6-31+G* optimized structures of (4,4)-BNNT-NH₃. Blue, yellow and grey colors represent N, B and H atoms, respectively. Bond lengths are in Å. Where BN bond distances are same in the vicinity of the active site, only one of those distances is shown.

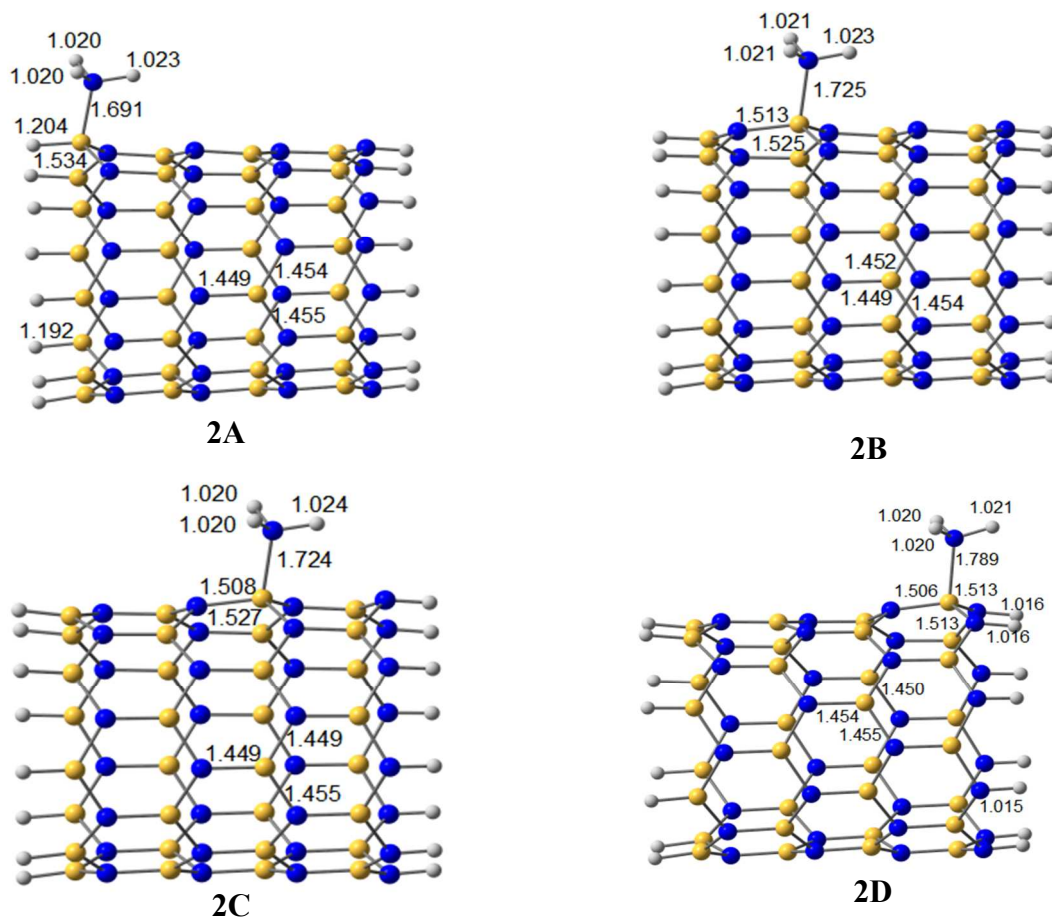


Fig. 2. BSSE corrected B3LYP/6-31+G* optimized structures of (8, 0)-BNNT-NH₃. Blue, yellow and grey colors represent N, B and H atoms, respectively. Bond lengths are in Å. Where BN bond distances are same in the vicinity of the active site, only one of those distances is shown.

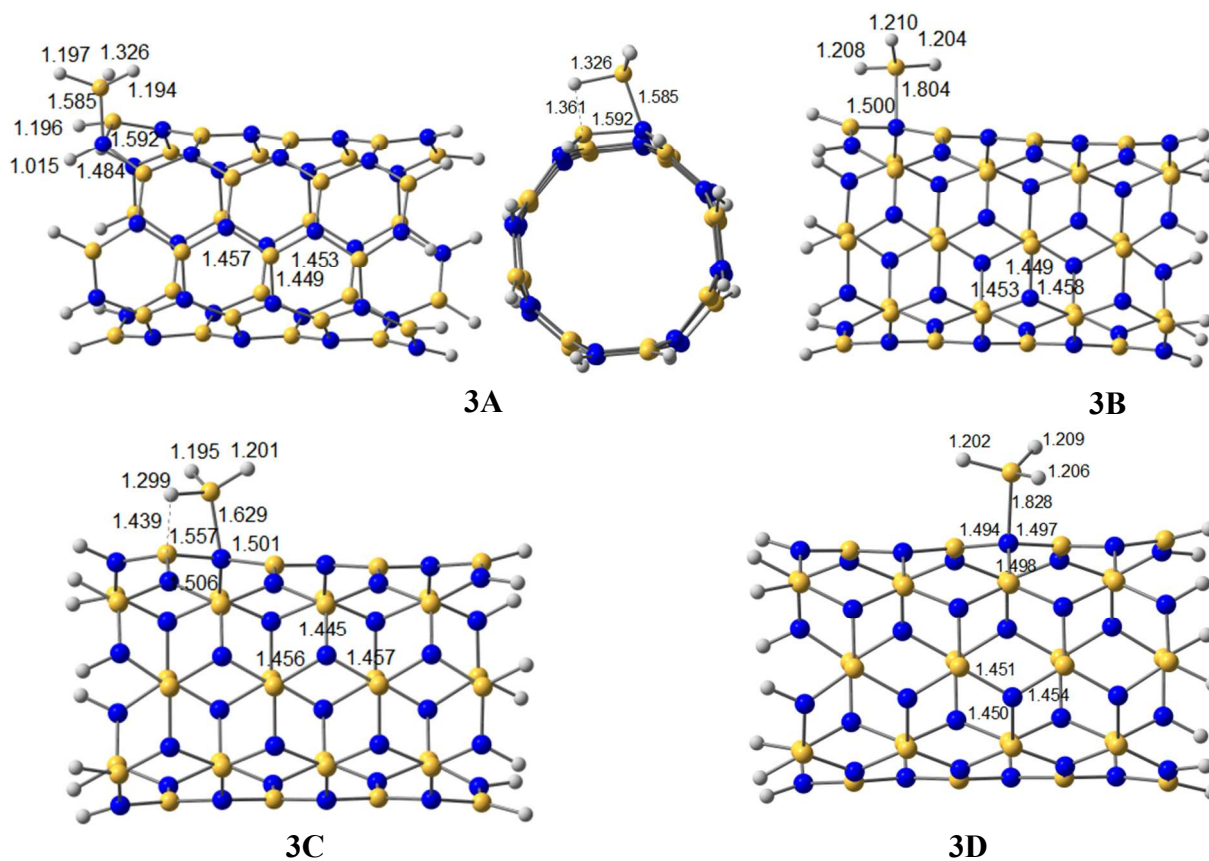


Fig. 3. BSSE corrected B3LYP/6-31+G* optimized structures of (4, 4)-BNNT-BH₃. Blue, yellow and grey colors represent N, B and H atoms, respectively. Bond lengths are in Å. Where BN bond distances are same in the vicinity of the active site, only one of those distances is shown.

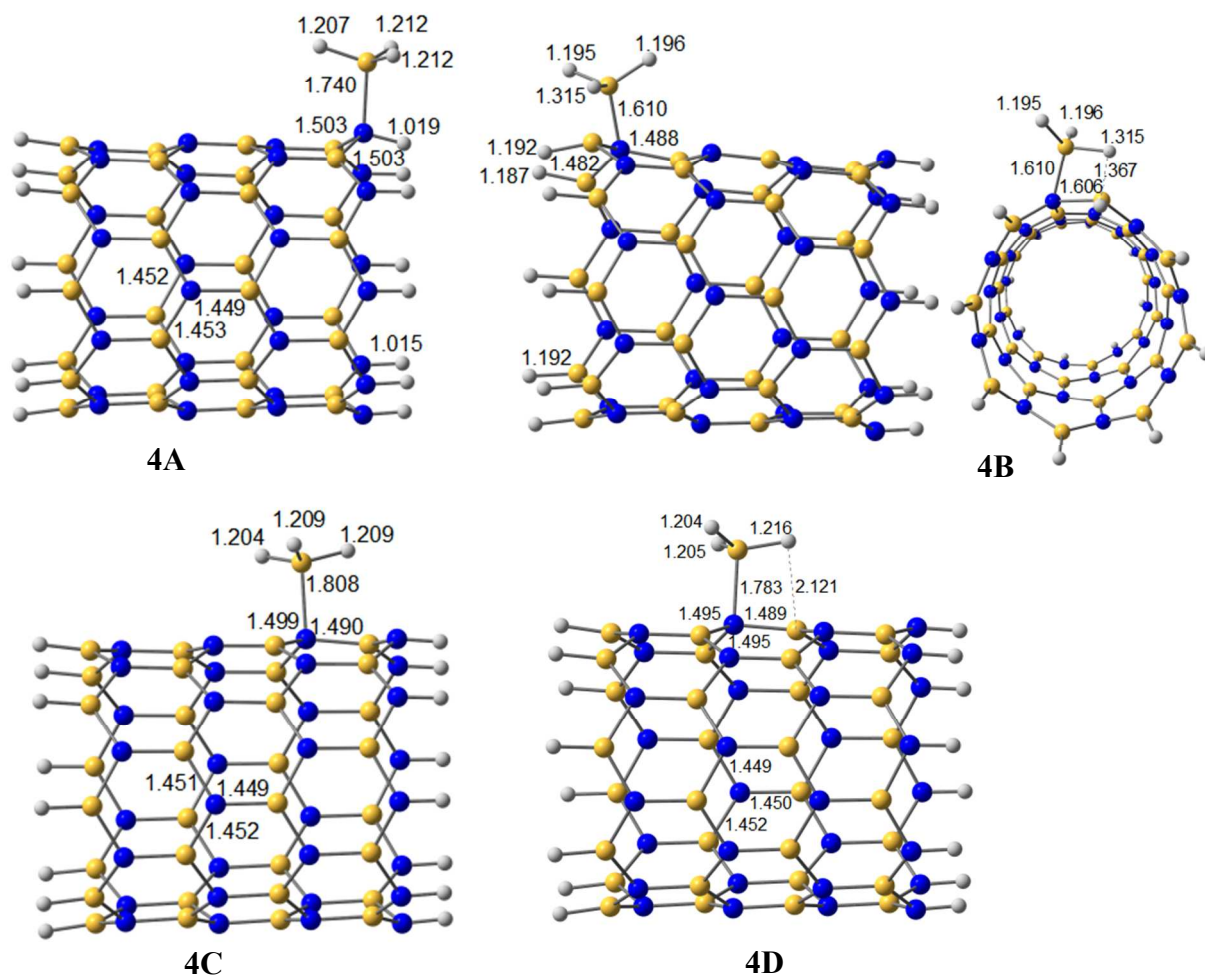


Fig. 4. BSSE corrected B3LYP/6-31+G* optimized structures of (8,0)-BNNT-BH₃. Blue, yellow and grey colors represent N, B and H atoms, respectively. Bond lengths are in Å. Where BN bond distances are same in the vicinity of the active site, only one of those distances is shown.

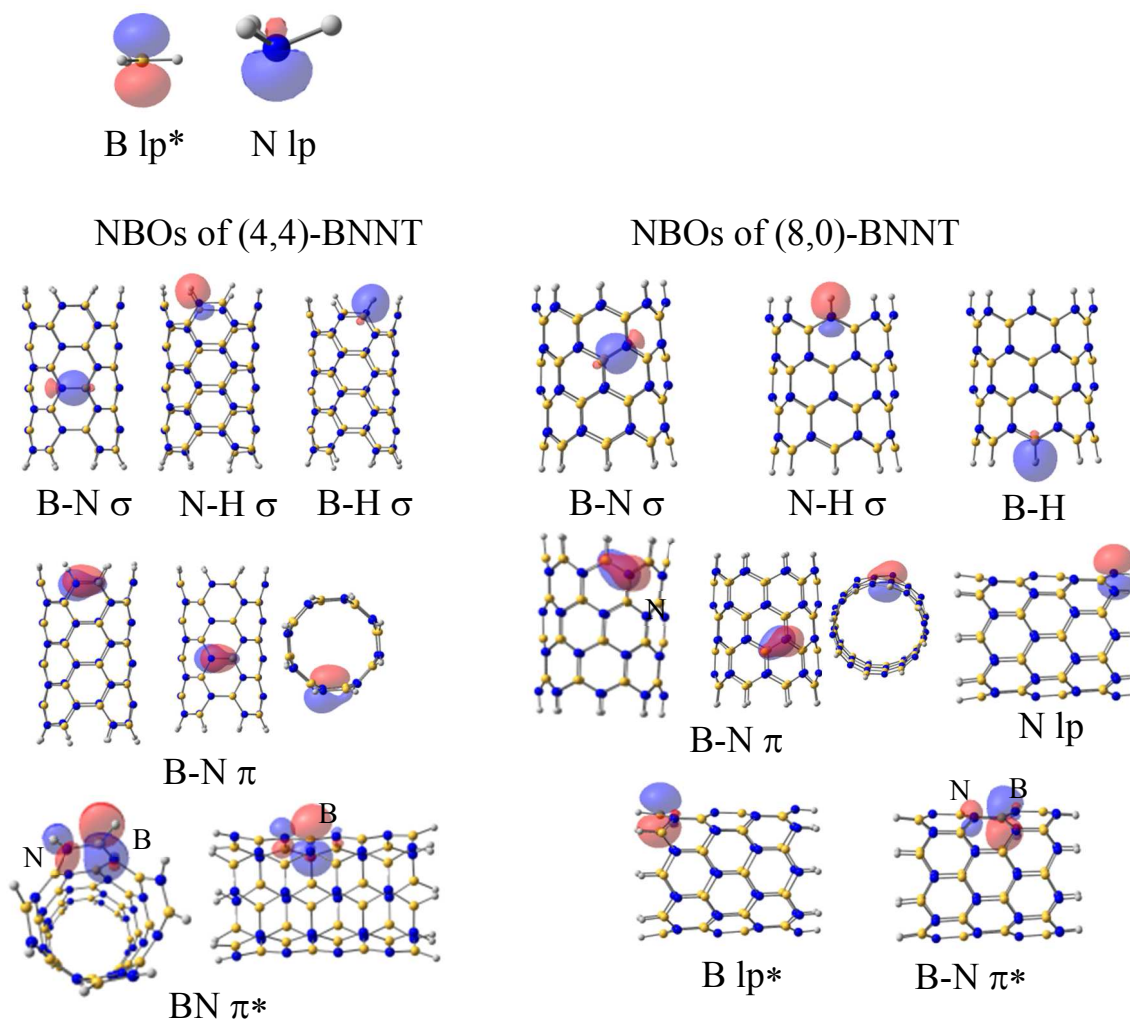


Fig. 5. Natural bond orbitals (NBO) of pristine BNNTs and lone pair of NH_3 and vacant π NBO of BH_3 . lp stands for lone pair, and * indicates antibonding/vacant NBOs.

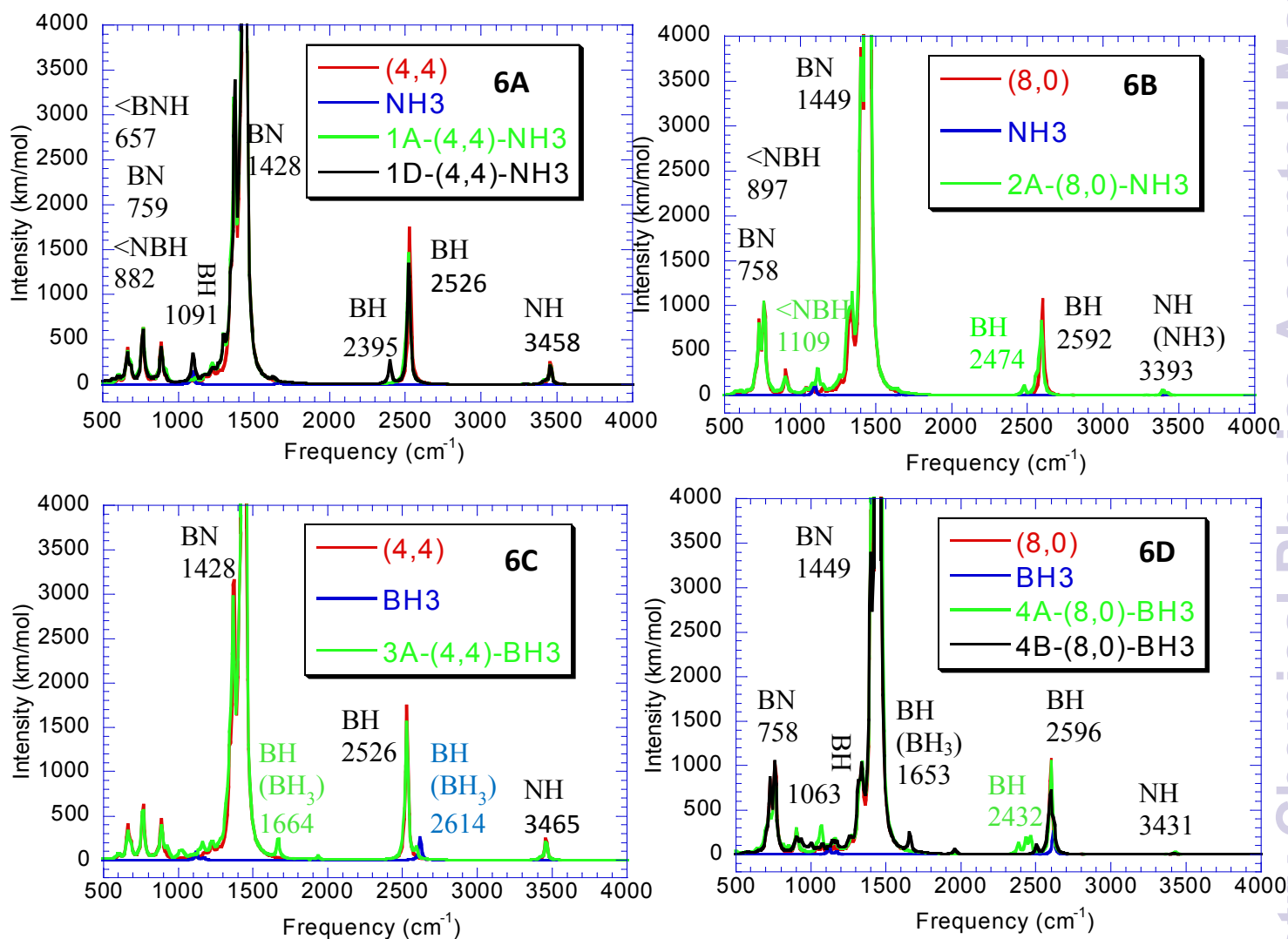


Fig. 6. IR spectra of most stable BNNT-NH₃/BH₃. Lorentzian broadening with fwhm of 20 cm⁻¹ was applied to each spectrum.

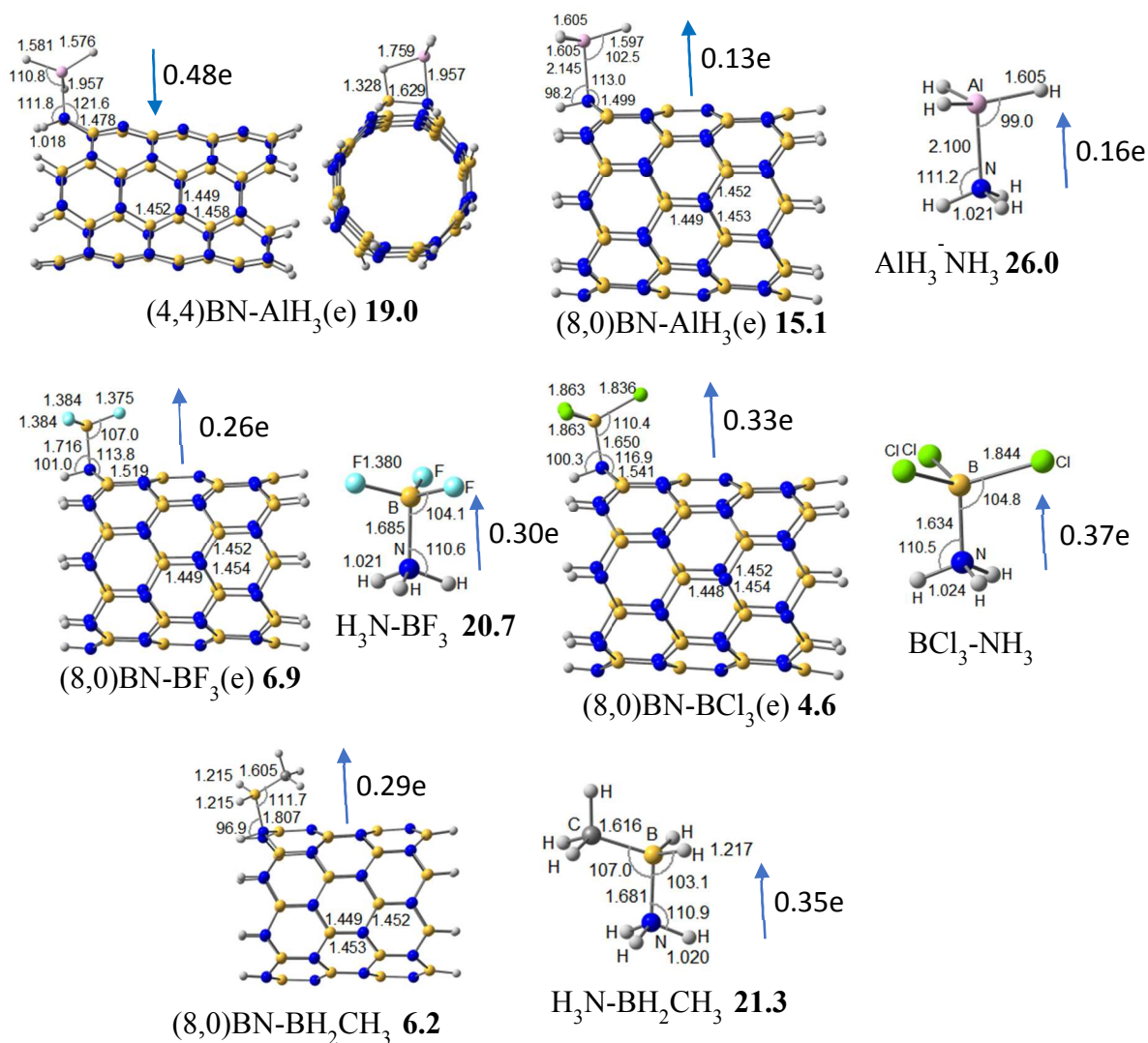


Fig. 7. B3LYP/6-31+G* optimized structures of $\text{H}_3\text{N-AIH}_3/\text{BF}_3/\text{BCl}_3/\text{BH}_2\text{CH}_3$ and corresponding BNNT- $\text{AIH}_3/\text{BF}_3/\text{BCl}_3/\text{BH}_2\text{CH}_3$. Bond lengths are in Å and angles are in degree. e and m stand for edge and middle adsorption sites of the tube, respectively. BSSE corrected adsorption energies (in kcal/mol) are given in bold and a positive value indicates attractive interaction between two units, otherwise interaction is repulsive. Most stable structures are show in this figure and other structures are given in Figure S9-S12. Electron transfer from or to BNNTs are shown by arrow with number of electron.

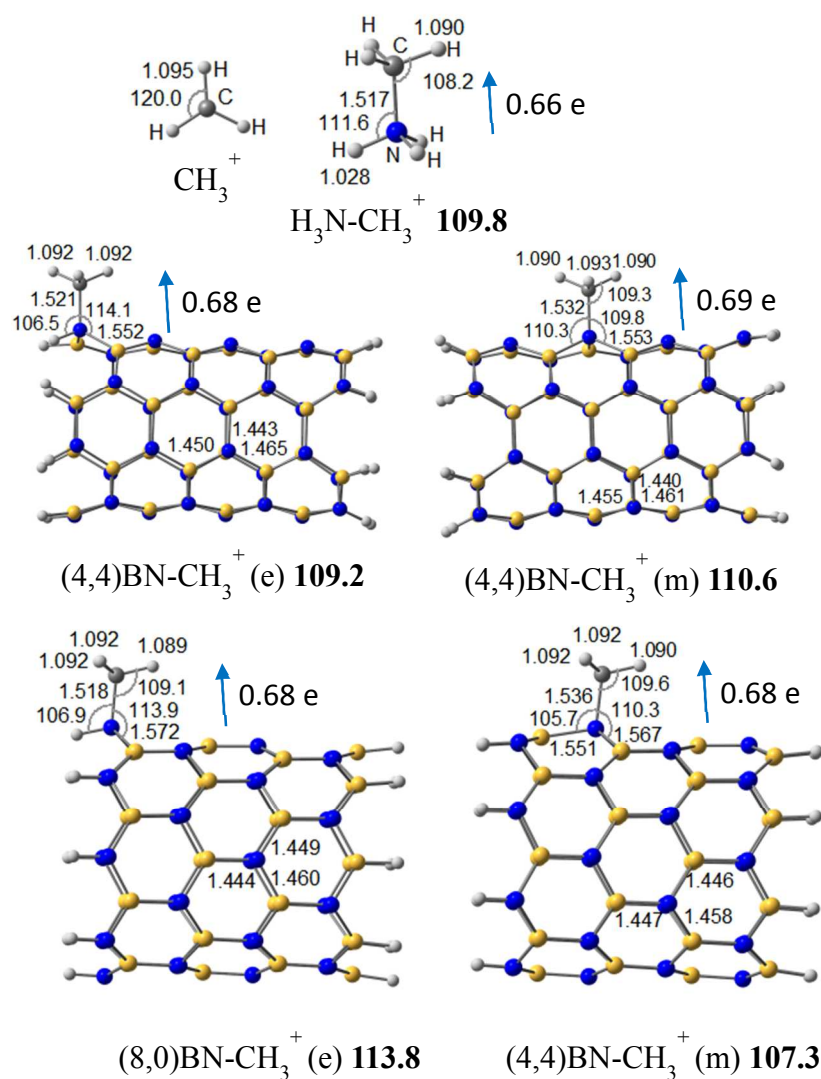


Fig. 8. B3LYP/6-31+G* optimized structures of $\text{H}_3\text{N}-\text{CH}_3^+$ and $\text{BNNT}-\text{CH}_3^+$. Bond lengths are in Å and angles are in degree. e and m stand for edge and middle adsorption sites of the tube, respectively. BSSE corrected adsorption energies (in kcal/mol) are given in bold and a positive value indicates attractive interaction among between two units. Electron transfer from or to BNNTs are shown by arrow with number of electron.

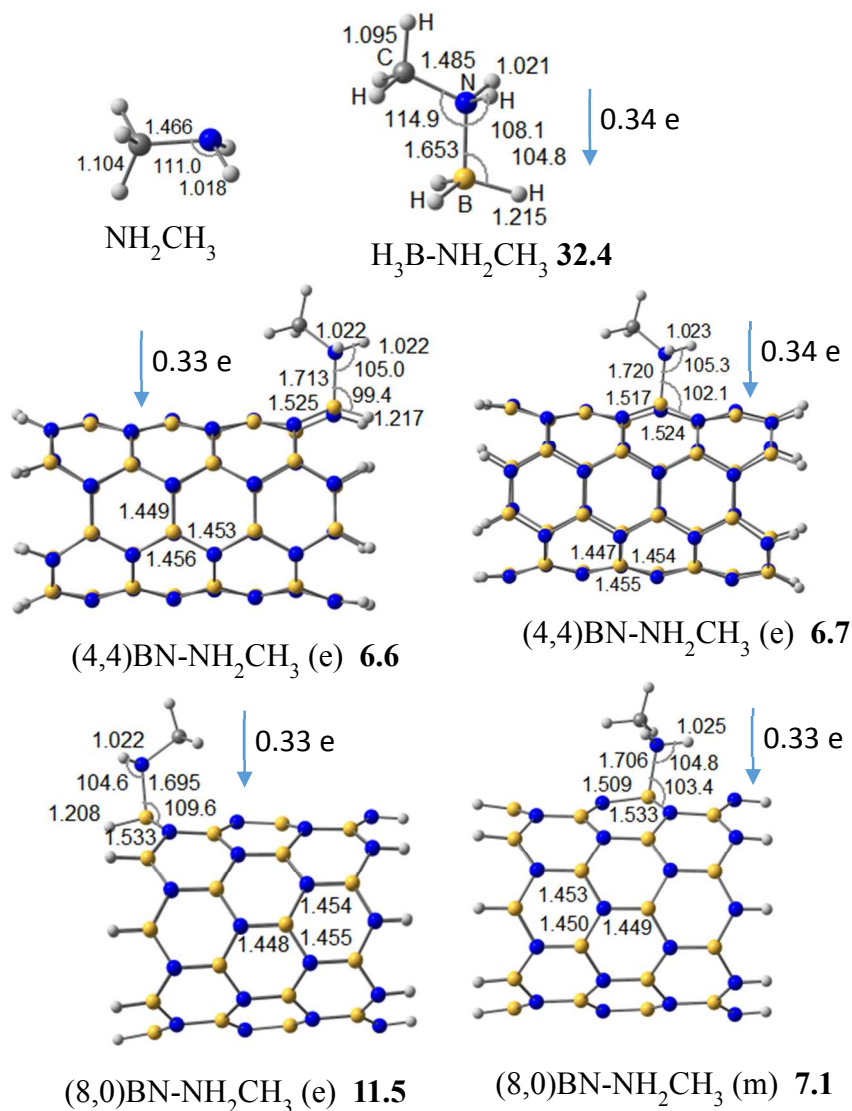


Fig. 9. B3LYP/6-31+G* optimized structures of $\text{H}_3\text{B-NH}_2\text{CH}_3$ and $\text{BN-NH}_2\text{CH}_3$. Bond lengths are in Å and angles are in degree. e and m stand for edge and middle adsorption sites of the tube, respectively. BSSE corrected adsorption energies (in kcal/mol) are given in bold and a positive value indicates attractive interaction among between two units, otherwise interaction is repulsive. Electron transfer from or to BNNTs are shown by arrow with number of electron.

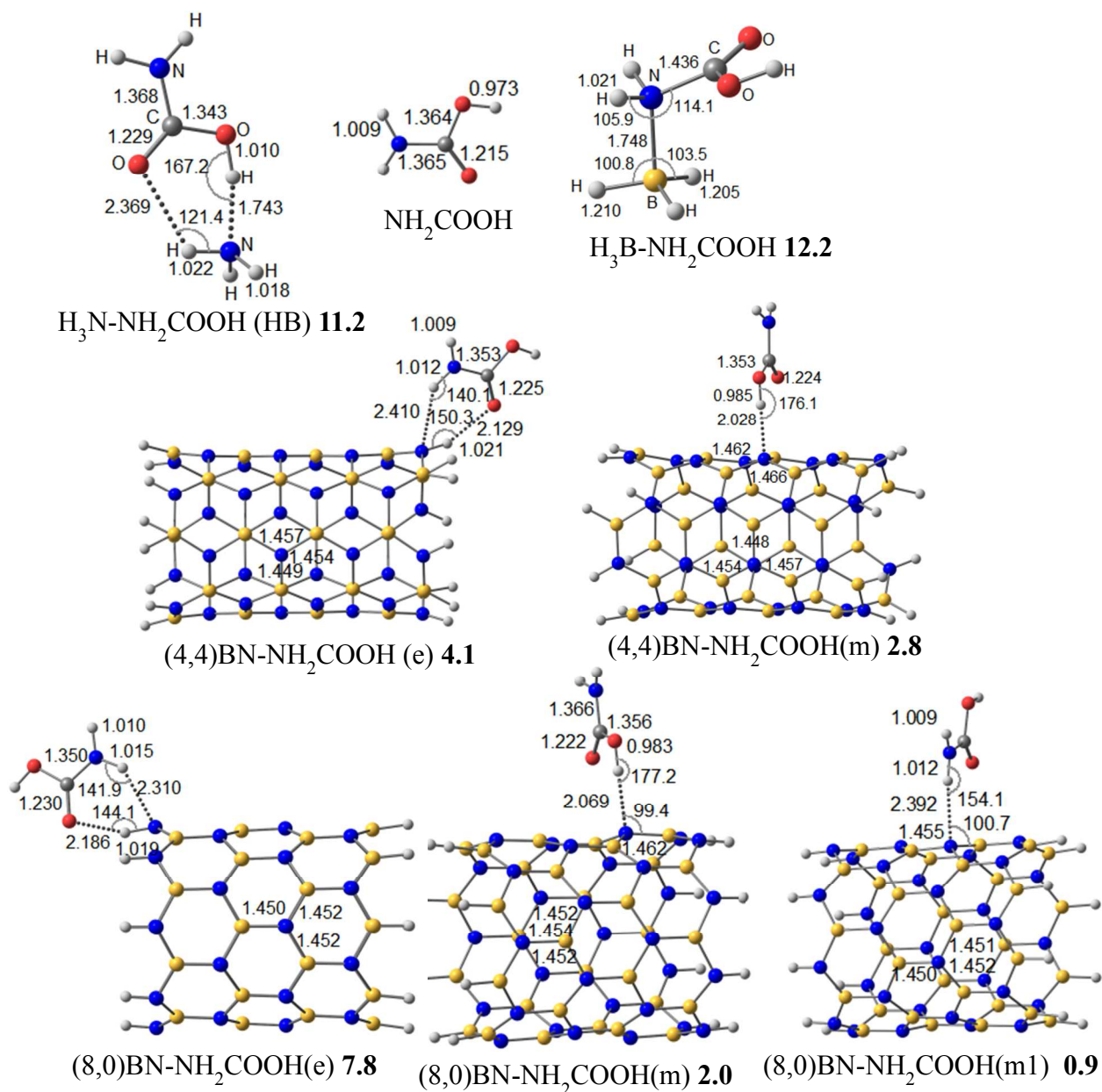


Fig. 10. B3LYP/6-31+G* optimized structures of BN-NH₂COOH. Bond lengths are in Å and angles are in degree. BSSE corrected adsorption energies (in kcal/mol) are given in bold and a positive value indicates attractive interaction among between two units, otherwise interaction is repulsive